PHILOSOPHICAL TRANSACTIONS OF THE ROYAL SOCIETY A MATHEMATICAL, PHYSICAL & ENGINEERING SCIENCES

Hele-Shaw Flows with Time-Dependent Free Boundaries Involving a Concentric Annulus

S. Richardson

Phil. Trans. R. Soc. Lond. A 1996 **354**, 2513-2553
doi: 10.1098/rsta.1996.0114

Hele-Shaw flows with time-dependent free boundaries involving a concentric annulus

By S. Richardson

Department of Mathematics and Statistics, University of Edinburgh, James Clerk Maxwell Building, King's Buildings, Mayfield Road, Edinburgh EH9 3JZ, UK

Contents

We consider the classical Hele-Shaw situation with two parallel planes separated by a narrow gap. A blob of Newtonian fluid is sandwiched between the planes and, initially, its plan-view occupies a doubly connected region, so that we physically have a fluid surrounding what we will refer to as an air hole. We seek to predict the evolution of the plan-view of the blob as fluid is added to or removed from the blob at specific injection or suction points, or as air is added to or removed from the air hole.

We suppose the relevant free boundary condition to be one of constant pressure, but allow different constant pressures to act along each free boundary. If we begin with a blob in the form of a concentric circular annulus, we obtain an analytic solution to describe its subsequent evolution when subjected to any pattern of injection or suction of fluid, or addition or removal of air, provided only that the plan-view of the blob either remains doubly connected or becomes simply connected as the air hole disappears. Since each state we can reach by this process may itself be regarded as an initial state for some subsequent motion, the class of problems we are thus able to solve is quite extensive.

The solutions are expressed in terms of conformal maps that have an explicit analytic form incorporating a finite number of parameters; in general, these parameters must be determined numerically by solving a finite set of transcendental equations. The efficacy of the procedure is illustrated by means of specific examples, chosen to exhibit a number of features of physical interest.

The development has an independent mathematical interest, for it involves the

Phil. Trans. R. Soc. Lond. A (1996) **354**, 2513–2553
Printed in Great Britain

solution of a nonlinear functional equation; we here deal only with the particular form of equation that arises in the present application, but generalizations can be handled by similar techniques. Also, the solutions are expressed in terms of functions which themselves have interesting properties. However, we do not pursue these mathematical questions in this paper.

1. Introduction

In an earlier paper (Richardson 1994), a framework was developed for the analysis of Hele-Shaw flows with time-dependent free boundaries in which the plan-view of the region occupied by the fluid was multiply connected; the pressure was supposed to be constant along each free boundary, but a different constant pressure may act along different free boundaries. Employing the familiar argument involving an averaging of the variables across the constant gap, we have a two-dimensional problem that can be posed in a Cartesian (x, y)-plane parallel to the planes bounding the Hele-Shaw cell by a projection onto this (x, y)-plane; we employ the usual complex variable $z = x + \mathrm{i}y$. With $D = D(t)$ the domain occupied by fluid at time t, supposed to be bounded, we define the Cauchy transform of D by

$$h(x, y; t) = h(x, y) = -\frac{1}{\pi} \iint_D \frac{\mathrm{d}\xi \, \mathrm{d}\eta}{\zeta - z}, \tag{1.1}$$

where $\zeta = \xi + \mathrm{i}\eta$. The explicit dependence of our functions on t will be suppressed in the notation, except where it seems essential to retain it for emphasis.

Denote by C_0 the outer boundary of D—that is, the portion of the boundary of D it has in common with the unbounded component of its complement. If D has connectivity N, there are also $N - 1$ closed curves that are inner boundaries of D; we denote a typical one by C_α and regard C_α as bounding an air hole in its interior. Then the Cauchy transform has the following crucial properties.

(i) The function $h(x, y)$ is continuous throughout the whole (x, y)-plane.

(ii) We have

$$h(x, y) = \begin{cases} h_e(z) & \text{for } z \text{ outside } C_0, \\ h_\alpha(z) & \text{for } z \text{ inside } C_\alpha, \\ \overline{z} - h_i(z) & \text{for } z \text{ in } D, \end{cases} \tag{1.2}$$

where $h_e(z)$, $h_\alpha(z)$ and $h_i(z)$ are functions that are analytic exterior to C_0, inside C_α, and interior to D, respectively; an overbar denotes the complex conjugate.

(iii) If fluid is injected into D at points $z = a_j$ for $j = 1, 2, \ldots, N$, with a total area $A_j(t)$ injected at a_j in the time interval from 0 to t and $A_j(t) < 0$ if fluid has actually been removed at a_j, then

$$h_e(z; t) = h_e(z; 0) + \frac{1}{\pi} \sum_{j=1}^{N} \frac{A_j(t)}{z - a_j}, \tag{1.3}$$

and

$$h_\alpha(z; t) = h_\alpha(z; 0) + \frac{1}{\pi} \sum_{j=1}^{N} \frac{A_j(t)}{z - a_j}. \tag{1.4}$$

From a given initial geometry and pattern of fluid injection or suction, we can still obtain different motions by endowing the air holes with different properties. We may suppose air vents to be so arranged that the pressure within C_α is maintained at the same value as that outside C_0, say; we might then expect that injection of fluid could result in C_α shrinking until the air hole within it disappears. In the absence of air vents, we may suppose the air within C_α to be effectively incompressible, so that the area within C_α must be maintained at a constant value. We may suppose the whole motion to be driven solely by the extraction or addition of air within C_α, so that the area enclosed by C_α is some given function of time; this scenario is particularly relevant when our real concern is to model flows in porous media that arise during gas recovery, when we wish to site any gas-producing well at the point where the gas pocket would disappear after shrinking. Whatever assumption we make about the air hole enclosed by C_α, relations (1.3) and (1.4) remain applicable; they require only that the pressure be constant along C_0 and the C_α, but different constant pressures may be relevant along C_0 and each C_α. Thus, to make the problem determinate, some extra conditions are required, one for each C_α, as discussed further by Richardson (1994). With these conditions included, properties (i), (ii) and (iii) above give a complete specification of the problem. Equations (1.3) and (1.4) tell us $h_e(z)$ and $h_\alpha(z)$ at any later time, but we do *not* need to know $h_i(z)$ in (1.2) then.

The functions $h_e(z)$ and $h_\alpha(z)$ in (1.2) are defined by (1.1) only outside C_0 and inside C_α, respectively, but we may contemplate their analytic continuation outside these regions; for example, we may be able to continue $h_\alpha(z)$ analytically into the region outside C_0 but, in general, it will *not* there be equal to $h_e(z)$.

If we begin injecting into a Hele-Shaw cell that is empty, we initially have fluid occupying disjoint circular discs centred on the injection points, but further injection will lead to a coalescence of blobs that may produce a multiply connected fluid region. Because the Cauchy transform evolves as a continuous function of t, and the definition (1.1) is still applicable when D is not a domain in the strict sense, but a union of disjoint domains, equations (1.3) and (1.4) are then appropriate for this multiply connected problem if we take $h_e(z;0) \equiv 0$ and $h_\alpha(z;0) \equiv 0$. In this case we see that, after analytic continuation, we *do* have that $h_e(z;t)$ and all the $h_\alpha(z;t)$ are equal, and this feature is a valuable simplification that was exploited by Richardson (1994).

The methods used in Richardson (1994) to solve particular problems were appropriate for doubly connected regions and, henceforth, we will restrict attention to such regions here. Thus the fluid domain D now has the outer boundary curve C_0 and just one inner boundary curve C_1—though we will also be interested in the degenerate situation as the air hole disappears and C_1 shrinks to a point. Correspondingly, we have just one function $h_\alpha(z)$ in (1.2), namely $h_1(z)$.

With a cut joining C_0 and C_1 within D to make D simply connected, we can map this cut region conformally onto a rectangle, the four points corresponding to the ends of the cut mapping to the corners of the rectangle. As shown in Richardson (1994), when $h_e(z) \equiv h_1(z)$ this conformal map is given by an elliptic function, provided the cut is chosen sensibly. We here consider cases where $h_e(z) \not\equiv h_1(z)$ when the map envisaged above is no longer given by an elliptic function; we must introduce generalizations of the standard elliptic functions if we wish to continue using a map onto a rectangle. Rather than pursue this approach, we choose to map the doubly connected domain D itself onto a concentric annulus and work with two simple special functions we define with our specific needs in mind.

Since the Cauchy transform is additive for disjoint domains, the Cauchy transform of a concentric annulus centred on the origin of the z-plane follows easily from that for a circular disc centred on the origin. If the area of the annulus is πr^2—that is, πr^2 is the area between its inner and outer boundaries—we find that

$$h_e(z) = r^2/z \qquad \text{and} \qquad h_1(z) \equiv 0. \tag{1.5}$$

Note that $h_e(z) \not\equiv h_1(z)$ here: a concentric circular annulus cannot be produced in an initially empty Hele-Shaw cell by injecting at a finite number of points, though it can be produced by injecting uniformly along a circular slit. Note, too, that (1.5) is relevant for *all* such annuli of area πr^2; we have already remarked that some other restriction concerned with the conditions pertaining to the air hole is necessary to fix the geometry. Here we may easily envisage the area of the hole being changed by the extraction or addition of air, when the ensuing motion simply involves the contraction or expansion of the annulus.

From the continuity of $h(x, y)$ and equations (1.2), we find that (1.5) implies

$$h_i(z) = \rho_{\mathrm{i}}^2/z, \tag{1.6}$$

where ρ_{i} is the radius of the inner circular boundary of the annulus. Thus $h_i(z)$ *does* change during the motion contemplated above. However, $h_i(z)$ plays a passive role in our analysis, and its precise form need never be determined.

Suppose now that an area πr_j^2 is injected at $z = a_j$ for $j = 1, 2, \ldots, N$ into a cell that already contains a concentric annulus of fluid described by (1.5). If this results in a fluid region that is doubly connected, then (1.3) and (1.4) imply that this region has

$$h_e(z) = \frac{r^2}{z} + \sum_{j=1}^{N} \frac{r_j^2}{z - a_j} \qquad \text{and} \qquad h_1(z) = \sum_{j=1}^{N} \frac{r_j^2}{z - a_j}\,. \tag{1.7}$$

Here, some of the r_j^2 may be negative, denoting that suction has actually taken place at $z = a_j$.

The remainder of the paper is concerned with the consequences of equations (1.7). In § 2, we show they imply that the function giving the conformal map of an annulus onto the doubly connected domain occupied by the fluid must satisfy a certain nonlinear functional equation; this functional equation replaces the linear difference equations characterizing the elliptic functions that arise when we treat problems for which $h_e(z) \equiv h_1(z)$. The solution to this nonlinear functional equation is obtained in § 3 and is expressed in terms of two functions that are defined in Appendix A; this appendix also contains a discussion of some of the basic properties of these functions. We also need some elementary results concerning loxodromic functions, and these are presented in Appendix B. Our solution of the nonlinear functional equation depends on the solution of a linear functional equation of q-difference form (or, more correctly, of q^2-difference form with the notation that proves most suitable for present purposes), and this is presented in Appendix C. The mathematical restrictions that arise from the physical assumptions we can make concerning the air hole are discussed in § 4.

With the principal mathematical difficulties dealt with, § 5 presents several specific solutions obtained using our results. The examples are given with only a minimum of mathematical details so that, aided by the illustrations, this section might be read and appreciated independently of the more mathematical sections. General computational aspects that arise when solving specific problems are discussed in § 6, but

PHILOSOPHICAL TRANSACTIONS OF THE ROYAL SOCIETY A MATHEMATICAL, PHYSICAL & ENGINEERING SCIENCES

the examples in § 5 also possess features that require a more detailed consideration. Some of them involve an air hole that ultimately shrinks to a point and disappears, and § 7 examines this degenerate situation. Others involve the formation of cusps in the free surface, but two quite different kinds of cusp appear and one must recognize this difference during the computations; this is discussed in § 8.

2. Derivation of the functional equation

The doubly connected domain D in the z-plane can be mapped conformally onto the annulus $q < |\zeta| < 1$ in the ζ-plane for some q satisfying $0 < q < 1$. With D given, we cannot, *a priori*, specify q; it is one of the parameters that must be determined subsequently and, as D varies with time, so does q. A situation in which the air hole vanishes corresponds to the limit $q \to 0$. We may suppose that the outer boundary C_0 of D corresponds to $|\zeta| = 1$ and the inner boundary C_1 of D corresponds to $|\zeta| = q$, and denote the function effecting the map by $z = f(\zeta)$. The specifications thus far fix the map only up to a rotation in the ζ-plane, but we will deal with this aspect later: the natural way to enforce uniqueness in a general situation will only become clear when we know more about the structure of $f(\zeta)$.

With functions $h_e(z)$ and $h_1(z)$ of the form (1.7) associated with D, the N points a_j all lie in D; let $\zeta = \gamma_j$ map to $z = a_j$ so that

$$f(\gamma_j) = a_j \qquad \text{for } j = 1, 2, \ldots, N. \tag{2.1}$$

The continuity of $h(x, y)$ and equation (1.2) imply that

$$h_1(z) + h_i(z) = \overline{z} \qquad \text{on } C_1.$$

Transforming to the ζ-plane, noting that $\zeta = q^2/\overline{\zeta}$ on $|\zeta| = q$, and using the form for $h_1(z)$ in (1.7), we obtain

$$\sum_{j=1}^{N} \frac{r_j^2}{f(\zeta) - a_j} + h_i(f(\zeta)) = \overline{f(q^2/\overline{\zeta})} \tag{2.2}$$

or, replacing ζ by $q^2/\overline{\zeta}$ and conjugating,

$$\sum_{j=1}^{N} \frac{r_j^2}{\overline{f(q^2/\overline{\zeta})} - \overline{a}_j} + \overline{h_i(f(q^2/\overline{\zeta}))} = f(\zeta). \tag{2.3}$$

Equations (2.2) and (2.3) are initially known to hold only on the circle $|\zeta| = q$, but with $f(\zeta)$ continuous for $q \leqslant |\zeta| \leqslant 1$ we see that, invoking the Schwarz reflection principle, they furnish the meromorphic continuation of $f(\zeta)$ into the annulus $q^2 < |\zeta| < q$. The term $h_i(f(\zeta))$ in (2.2) is analytic for $q < |\zeta| < 1$, so the term

$$\overline{h_i(f(q^2/\overline{\zeta}))}$$

in (2.3) is analytic for $q^2 < |\zeta| < q$; the singularities of $f(\zeta)$ in $q^2 < |\zeta| < q$ are dictated by the terms in the sum on the left-hand side of (2.3), so that $f(\zeta)$ must have a pole at $\zeta = q^2/\overline{\gamma}_j$ for $j = 1, 2, \ldots, N$. It is, in fact, more convenient to express the formulae we need in terms of the function

$$\overline{f(q^2/\overline{\zeta})}$$

appearing on the right-hand side of (2.2). This has poles at $\zeta = \gamma_j$ for $j = 1, 2, \ldots, N$

and these must be *simple* poles because $f'(\gamma_j) \neq 0$: we know that $f(\zeta)$ is *univalent* for $q < |\zeta| < 1$, and all the γ_j are within this annulus. Let β_j be the residue of

$$\overline{f(q^2/\bar{\zeta})}$$

at $\zeta = \gamma_j$, so we have

$$\overline{f(q^2/\bar{\zeta})} = \frac{\beta_j}{\zeta - \gamma_j} + O(1) \qquad \text{as } \zeta \to \gamma_j. \tag{2.4}$$

This means that $f(\zeta)$ itself has a simple pole of residue $-q^2\overline{\beta}_j/\overline{\gamma}_j^2$ at $\zeta = q^2/\overline{\gamma}_j$; these expressions relating to $f(\zeta)$ are rather less elegant than the corresponding ones for

$$\overline{f(q^2/\bar{\zeta})}$$

incorporated into (2.4) but, comparing residues on both sides of (2.2), we find that the choice in (2.4) leads to the simple equations

$$\beta_j f'(\gamma_j) = r_j^2 \qquad \text{for } j = 1, 2, \ldots, N. \tag{2.5}$$

The continuity of $h(x, y)$ and equation (1.2) imply that

$$h_e(z) + h_i(z) = \overline{z} \qquad \text{on } C_0.$$

Transforming to the ζ-plane, noting that $\zeta = 1/\bar{\zeta}$ on $|\zeta| = 1$, and using the form for $h_e(z)$ in (1.7), we obtain an equation similar to (2.3), namely

$$\frac{r^2}{\overline{f(1/\bar{\zeta})}} + \sum_{j=1}^{N} \frac{r_j^2}{\overline{f(1/\bar{\zeta})} - \overline{a}_j} + \overline{h_i(f(1/\bar{\zeta}))} = f(\zeta). \tag{2.6}$$

With $f(\zeta)$ first continued using (2.3) so that we know it to be meromorphic in the annulus $q^2 < |\zeta| < 1$, equation (2.6) furnishes its meromorphic continuation into the annulus $1 < |\zeta| < q^{-2}$. In fact, equations (2.3) and (2.6) together now give the meromorphic continuation of $f(\zeta)$ into the entire region $|\zeta| > 0$. This process can be carried out somewhat more efficiently using an equation that can be derived from (2.3) and (2.6): replacing ζ by $q^2\zeta$ in (2.3) and subtracting the result from (2.6), we find that

$$f(\zeta) - f(q^2\zeta) = \frac{r^2}{\overline{f(1/\bar{\zeta})}}. \tag{2.7}$$

This nonlinear functional equation satisfied by the mapping function $f(\zeta)$ is central to our approach. Knowing the singularities of $f(\zeta)$ in the annulus $q^2 < |\zeta| < 1$ that are implied by the meromorphic continuation effected by (2.3), equation (2.7) automatically forces $f(\zeta)$ to have the singularities in the annulus $1 < |\zeta| < q^{-2}$ that are implied by the meromorphic continuation effected by (2.6).

In this respect, we note an important difference between the continuations resulting from (2.3) and (2.6) which arises from the first term on the left-hand side of (2.6) that has no analogue in (2.3). Beginning with injection into our basic annulus in the z-plane, we may eventually reach a situation where fluid moves to cover the origin $z = 0$. Then a zero of $f(\zeta)$ has moved across $|\zeta| = q$ into the annulus $q < |\zeta| < 1$, and (2.6) implies that a simple pole of $f(\zeta)$ has moved across $|\zeta| = q^{-1}$ into the annulus $1 < |\zeta| < q^{-1}$. Thus, while (2.3) tells us *precisely* what singularities $f(\zeta)$ must have in the annulus $q^2 < |\zeta| < 1$, there is, *a priori*, a degree of uncertainty about the

behaviour of $f(\zeta)$ in the annulus $q < |\zeta| < q^{-1}$ implied by (2.6). For this reason, we concentrate on the annulus $q^2 < |\zeta| < 1$; equation (2.7) then forces $f(\zeta)$ to behave as necessary outside it. (The difficulties of dealing with (2.6) directly are compounded if, having injected so that the origin is covered, we decide to inject more fluid there; then the first term on the left-hand side of (2.6) contributes to a singularity that is already forced by a term in the sum. With our approach, such a coalescence causes no problems, but see later comments on this point.)

Summing up, we need a solution $f(\zeta)$ of the nonlinear functional equation (2.7) that is analytic and univalent in the annulus $q < |\zeta| < 1$, whose only singularities in the annulus $q^2 < |\zeta| < 1$ are simple poles at the points $\zeta = q^2/\overline{\gamma}_j$ for $j = 1, 2, \ldots, N$, and which is such that conditions (2.1) and (2.5) are satisfied, where the parameters β_j in (2.5) are defined by (2.4). We know that we can impose a further condition on $f(\zeta)$ to fix the orientation in the ζ-plane, and a second extra restriction arises from the physical assumptions made concerning the air hole; with these additions, we will show that the function $f(\zeta)$ is uniquely determined by this prescription.

3. Solution of the functional equation

Our solution of the nonlinear functional equation (2.7) will be expressed in terms of the functions $F(z)$ and $G(z)$ defined in Appendix A. We also need some results concerning loxodromic functions given in Appendix B, and exploit the solution of the linear functional equation presented in Appendix C.

Define

$$g(\zeta) = f(\zeta)\overline{f(q^2/\overline{\zeta})}. \tag{3.1}$$

Since $f(\zeta)$ is meromorphic for $\zeta \neq 0$, so is $g(\zeta)$. We know that the only singularities of $f(\zeta)$ in the annulus $q^2 < |\zeta| < 1$ are at $\zeta = q^2/\overline{\gamma}_j$ for $j = 1, 2, \ldots, N$, and these are simple poles; the behaviour of $f(\zeta)$ near these poles is described by equation (2.4), and these poles are, in fact, all in the annulus $q^2 < |\zeta| < q$. It follows that $g(\zeta)$ has just $2N$ simple poles in the annulus $q^2 < |\zeta| < 1$ at the points $\zeta = \gamma_j$ and $\zeta = q^2/\overline{\gamma}_j$ for $j = 1, 2, \ldots, N$. From (2.1), (2.4) and (3.1) we find, in particular, that

$$g(\zeta) = \frac{a_j \beta_j}{\zeta - \gamma_j} + O(1) \qquad \text{as } \zeta \to \gamma_j. \tag{3.2}$$

We remark in Appendix B that, in the theory of loxodromic and elliptic functions, awkward placing of special points can produce exceptional circumstances that really require separate treatment but, after some initial comment, it is traditional not to complicate a presentation by repeating such qualifications. Similar difficulties arise here, and we adopt the same attitude. For example, we have seen that we may have a situation where we are injecting at the origin, so that $a_j = 0$ for one particular j. Relation (3.2) implies that $\zeta = \gamma_j$ is then actually *not* a pole of $g(\zeta)$—and neither is $\zeta = q^2/\overline{\gamma}_j$. Nothing is amiss with our equations, but it is the verbal description that becomes inadequate; so far as (3.2) is concerned we just have 'a simple pole with zero residue'. However, an injection point at the origin will cause difficulties in some of our later equations, and there are steps in the argument that should then be amended. To keep our account free from such distractions, we suppose that $a_j \neq 0$ for all j.

PHILOSOPHICAL TRANSACTIONS OF THE ROYAL SOCIETY A MATHEMATICAL, PHYSICAL & ENGINEERING SCIENCES

Now multiply equation (2.7) through by $\overline{f(1/\bar{\zeta})}$; we obtain

$$f(\zeta)\overline{f(1/\bar{\zeta})} - f(q^2\zeta)\overline{f(1/\bar{\zeta})} = r^2. \tag{3.3}$$

Replacing ζ by $1/\bar{\zeta}$ in this and conjugating, we have

$$f(\zeta)\overline{f(1/\bar{\zeta})} - f(\zeta)\overline{f(q^2/\bar{\zeta})} = r^2$$

which, noting the definition of $g(\zeta)$ in (3.1), is

$$g(\zeta) + r^2 = f(\zeta)\overline{f(1/\bar{\zeta})}. \tag{3.4}$$

Comparison of (3.3) and (3.4) now shows that

$$g(\zeta) = f(q^2\zeta)\overline{f(1/\bar{\zeta})}. \tag{3.5}$$

But if we replace ζ by $q^2\zeta$ in (3.1), its right-hand side becomes equal to the right-hand side of (3.5), so

$$g(\zeta) = g(q^2\zeta)\,: \tag{3.6}$$

the function $g(\zeta)$ is loxodromic, as defined by (B 1), with $q^2 < |\zeta| \leqslant 1$ as fundamental annulus. From (3.4), we also see that

$$g(\zeta) = \overline{g(1/\bar{\zeta})}, \tag{3.7}$$

so $g(\zeta)$ is a loxodromic function with the additional symmetry enshrined in (B 10); this is in accord with our observations concerning the distribution of the poles of $g(\zeta)$.

Since $g(\zeta)$ has $2N$ poles in the fundamental annulus, it must also have $2N$ zeros there. From the structure of $g(\zeta)$ displayed in its definition (3.1) as a product, N of those zeros must be zeros of $f(\zeta)$, say at $\zeta = \delta_j$ for $j = 1, 2, \ldots, N$, while the others are zeros of

$$\overline{f(q^2/\bar{\zeta})}$$

at $\zeta = q^2/\bar{\delta}_j$ for $j = 1, 2, \ldots, N$. Now, $f(\zeta)$ gives a conformal map of the annulus $q < |\zeta| < 1$, so all its poles are in $q^2 < |\zeta| < q$, and all the poles of

$$\overline{f(q^2/\bar{\zeta})}$$

are in $q < |\zeta| < 1$. If we imagine injection into an initial annulus, then we must certainly have all the zeros of $f(\zeta)$ in the annulus $q^2 < |\zeta| < q$ to begin with, and all the zeros of

$$\overline{f(q^2/\bar{\zeta})}$$

are in the annulus $q < |\zeta| < 1$. Thus *there is no possibility of any cancellation occurring between zeros and poles* when $g(\zeta)$ is formed via the product in (3.1). As this injection progresses, when fluid moves to cover the origin one (and only one) zero $\zeta = \delta_j$ of $f(\zeta)$ moves into the annulus $q < |\zeta| < 1$ (this can occur while $|\delta_j|$ and q are both decreasing, the zero being overtaken by the shrinking inner boundary $|\zeta| = q$ of the annulus), while the corresponding zero $\zeta = q^2/\bar{\delta}_j$ of

$$\overline{f(q^2/\bar{\zeta})}$$

moves into $q^2 < |\zeta| < q$; at the instant of covering, these simple zeros coalesce to give a double zero of $g(\zeta)$ on $|\zeta| = q$. If, and only if, we subsequently introduce

injection at the origin after it has been covered by fluid do we have cancellation between zeros and poles in (3.1), and we have already remarked that we will suppose this not to be the case to avoid complicating the presentation. It is at this juncture that a development with injection at the origin would begin to differ significantly from that being recorded, for the function $g(\zeta)$ would then have $2N-2$ poles in the fundamental annulus instead of $2N$: note that we must have $N > 1$ in such circumstances.

Using formula (B 9), we now see that $g(\zeta)$ must have a representation of the form

$$g(\zeta) = C\prod_{j=1}^{N}\frac{F(\zeta/\delta_j)F(\overline{\delta}_j\zeta/q^2)}{F(\zeta/\gamma_j)F(\overline{\gamma}_j\zeta/q^2)}, \tag{3.8}$$

where C is a constant that must be real because of (3.7). Moreover, the zeros and poles of $g(\zeta)$ are subject to the restriction

$$\frac{\delta_1\delta_2\ldots\delta_N}{\overline{\delta}_1\overline{\delta}_2\ldots\overline{\delta}_N} = \frac{\gamma_1\gamma_2\cdots\gamma_N}{\overline{\gamma}_1\overline{\gamma}_2\cdots\overline{\gamma}_N}. \tag{3.9}$$

We have written this in a form that reflects its origin in (B 8), but observe that it constitutes a condition affecting only the arguments of the δ_j and γ_j, and not their moduli.

The function $g(\zeta)+r^2$ is also loxodromic, and enjoys the same additional symmetry (3.7) as does $g(\zeta)$. It has the same $2N$ poles in the fundamental annulus $q^2 < |\zeta| \leqslant 1$ as has $g(\zeta)$; we denote the $2N$ zeros of $g(\zeta)+r^2$ in this annulus by $\zeta = \epsilon_j$ and $\zeta = q^2/\overline{\epsilon}_j$ for $j = 1, 2, \ldots, N$. Thus

$$g(\zeta)+r^2 = D\prod_{j=1}^{N}\frac{F(\zeta/\epsilon_j)F(\overline{\epsilon}_j\zeta/q^2)}{F(\zeta/\gamma_j)F(\overline{\gamma}_j\zeta/q^2)}, \tag{3.10}$$

where D is a real constant, and

$$\frac{\epsilon_1\epsilon_2\ldots\epsilon_N}{\overline{\epsilon}_1\overline{\epsilon}_2\ldots\overline{\epsilon}_N} = \frac{\gamma_1\gamma_2\cdots\gamma_N}{\overline{\gamma}_1\overline{\gamma}_2\cdots\overline{\gamma}_N}. \tag{3.11}$$

We now note an apparent contradiction: the functions $g(\zeta)$ and $g(\zeta)+r^2$ cannot have any zeros in common (for $r^2 \neq 0$), but formulae (3.1) and (3.4) express them both as products with $f(\zeta)$ as one factor. This is why we were at pains to point out that there can be no cancellation of zeros and poles in the product in (3.1) with no injection at the origin—such cancellation *must* occur in the product in (3.4).

If we eliminate

$$\overline{f(1/\overline{\zeta})}$$

between equations (3.4) and (3.5), we obtain

$$f(q^2\zeta) = \frac{g(\zeta)}{g(\zeta)+r^2}\, f(\zeta). \tag{3.12}$$

The quotient involving $g(\zeta)$ here is a loxodromic function whose representation follows from (3.8) and (3.10). Equation (3.12) is thus a linear functional equation for $f(\zeta)$ of the kind discussed in Appendix C. From (C 5), we see that $f(\zeta)$ must have a representation of the form

$$f(\zeta) = L_1(\zeta)\frac{F(\zeta/\alpha_1)}{F(\zeta/\alpha_2)}\prod_{j=1}^{N}\frac{G(\zeta/\delta_j)G(\overline{\delta}_j\zeta/q^2)}{G(\zeta/\epsilon_j)G(\overline{\epsilon}_j\zeta/q^2)} \tag{3.13}$$

in terms of the functions $F(z)$ and $G(z)$ defined in Appendix A, where $L_1(\zeta)$ is loxodromic, while α_1 and α_2 are constants whose ratio is all that is relevant.

Now, in the annulus $q^2 < |\zeta| \leqslant 1$ the only zeros of $f(\zeta)$ are to be at $\zeta = \delta_j$ for $j = 1, 2, \ldots, N$, and the only poles are to be at $\zeta = q^2/\overline{\gamma}_j$ for $j = 1, 2, \ldots, N$, and the combination of G-functions appearing in (3.13) is not consistent with this requirement, as written. However, we can use (A 6) to adjust the arguments of these functions to cure this defect; we need to multiply the argument of the first G-function in the numerator of each factor of the product in (3.13) by q^4, and the argument of the other G-functions by q^2. Equation (A 6) then produces five F-functions from each factor but, because of (3.9) and (3.11), the product involving four of these is loxodromic and can be absorbed into $L_1(\zeta)$. We can thus rewrite (3.13) as

$$f(\zeta) = L_2(\zeta)\frac{F(\zeta/\alpha_1)}{F(\zeta/\alpha_2)}\prod_{j=1}^{N}\frac{G(q^4\zeta/\delta_j)G(\overline{\delta}_j\zeta)}{G(q^2\zeta/\epsilon_j)G(\overline{\epsilon}_j\zeta)}\frac{1}{F(q^2\zeta/\delta_j)}, \tag{3.14}$$

where $L_2(\zeta)$ is loxodromic. The combination of G-functions now has just simple zeros at $\zeta = \delta_j$ for $j = 1, 2, \ldots, N$ and no poles within the annulus $q^2 < |\zeta| \leqslant 1$, but our plans have been thwarted by the appearance of the F-functions in the factors of the product: these produce poles at $\zeta = \delta_j$ for $j = 1, 2, \ldots, N$ when we need them at $\zeta = q^2/\overline{\gamma}_j$. But, if $N > 1$, consider

$$\frac{F(q^2\zeta/\delta_1)}{F(\zeta/\alpha_3)}\prod_{j=2}^{N}\frac{F(q^2\zeta/\delta_j)}{F(\overline{\gamma}_j\zeta)}.$$

(If $N = 1$ the argument is simpler: just take $\alpha_1 = \delta_1/q^2$.) We can choose α_3 so that the relevant form of condition (B 8) is satisfied and this function is loxodromic, and then factor this expression from the loxodromic function $L_2(\zeta)$ in (3.14). We may then choose $\alpha_1 = \alpha_3$ so that we have effectively rearranged the representation (3.14) to remove the N poles at $\zeta = \delta_j$ for $j = 1, 2, \ldots, N$ and introduced the $N - 1$ poles at $\zeta = q^2/\overline{\gamma}_j$ for $j = 2, \ldots, N$. But now, to have the pole at $\zeta = q^2/\overline{\gamma}_1$, the point $\zeta = \alpha_2$ must be equivalent to $\zeta = q^2/\overline{\gamma}_1$—that is, α_2 is equal to $q^2/\overline{\gamma}_1$ multiplied by some integer power of q^2. From (A 3), we see that $F(\zeta/\alpha_2)$ then differs from $F(\overline{\gamma}_1\zeta)$ only by a factor that is an integer power of ζ times an irrelevant constant. Thus we find that (3.14) must be of the form

$$f(\zeta) = \zeta^n L_3(\zeta)\prod_{j=1}^{N}\frac{G(q^4\zeta/\delta_j)G(\overline{\delta}_j\zeta)}{G(q^2\zeta/\epsilon_j)G(\overline{\epsilon}_j\zeta)}\frac{1}{F(\overline{\gamma}_j\zeta)} \tag{3.15}$$

for some loxodromic function $L_3(\zeta)$ and some integer n. Now the combination of F-functions and G-functions in (3.15) has just the poles (and zeros) in the annulus $q^2 < |\zeta| \leqslant 1$ that we know $f(\zeta)$ to have, so the loxodromic function $L_3(\zeta)$ must, in fact, be a constant and

$$f(\zeta) = E\zeta^n\prod_{j=1}^{N}\frac{G(q^4\zeta/\delta_j)G(\overline{\delta}_j\zeta)}{G(q^2\zeta/\epsilon_j)G(\overline{\epsilon}_j\zeta)}\frac{1}{F(\overline{\gamma}_j\zeta)}, \tag{3.16}$$

where E is some constant.

What can we say about n? This is determined by the requirement that $f(\zeta)$ be univalent for $q < |\zeta| < 1$, and to discover the implications of this we consider the

motion to evolve from an initial state with just the basic concentric annulus in the z-plane. Then $f(\zeta)$ must degenerate to a constant multiple of ζ and, from (3.1), $g(\zeta)$ becomes a constant. Thus there must be a coalescence of zeros and poles in formula (3.8). Now all the points $\zeta = \gamma_j$ lie in $q < |\zeta| < 1$, and all the points $\zeta = \delta_j$ are in $q^2 < |\zeta| < q$, so the zeros at $\zeta = \delta_j$ must coalesce with the poles at $\zeta = q^2/\overline{\gamma}_j$. In fact, we have not yet introduced any means of distinguishing between the N points $\zeta = \delta_j$. Equation (2.1) associates γ_j with a_j for each $j = 1, 2, \ldots, N$, and we can now suppose the labelling to be so chosen that δ_j coincides with $q^2/\overline{\gamma}_j$ for each $j = 1, 2, \ldots, N$ when we have the degenerate situation with the basic annulus.

With the annular configuration, $g(\zeta) + r^2$ is also constant, so the zeros and poles in formula (3.10) must coalesce too. We can now choose the labelling of the points ϵ_j so that ϵ_j coincides with $q^2/\overline{\gamma}_j$ for each $j = 1, 2, \ldots, N$. Note that, thus far, we have not even distinguished between the zeros of $g(\zeta) + r^2$ at $\zeta = \epsilon_j$ and $\zeta = q^2/\overline{\epsilon}_j$; formula (3.16) remains unchanged if we substitute $q^2/\overline{\epsilon}_j$ for ϵ_j. By contrast, there *has* been a distinction between the zeros of $g(\zeta)$ at $\zeta = \delta_j$ and $\zeta = q^2/\overline{\delta}_j$; the former are zeros of $f(\zeta)$, while the latter are zeros of

$$\overline{f(q^2/\overline{\zeta})}.$$

If we let $\delta_j \to q^2/\overline{\gamma}_j$ and $\epsilon_j \to q^2/\overline{\gamma}_j$ for each $j = 1, 2, \ldots, N$ we find, using (A 6), that formula (3.16) collapses to $f(\zeta) = E\zeta^n$, so that we must then have $n = 1$ for univalence. Since a continuous evolution cannot change an integer, we finally deduce that

$$f(\zeta) = E\zeta \prod_{j=1}^{N} \frac{G(q^4\zeta/\delta_j)G(\overline{\delta}_j\zeta)}{G(q^2\zeta/\epsilon_j)G(\overline{\epsilon}_j\zeta)} \frac{1}{F(\overline{\gamma}_j\zeta)}, \tag{3.17}$$

where E is a constant—and we now see the natural condition to apply to achieve uniqueness of the mapping and fix the orientation in the ζ-plane: we suppose E to be real and positive.

Formula (3.17) contains two real parameters E and q, and $3N$ complex parameters γ_j, δ_j and ϵ_j; to determine these, we evidently need more equations than the $2N$ complex equations (2.1) and (2.5), with (2.4) defining β_j, and the one real equation, to be discussed in § 4, that relates to properties of the air hole. In fact, further restrictions are easy to find; since $g(\zeta)$ vanishes for $\zeta = \delta_j$, setting $\zeta = \delta_j$ in (3.10) gives us N complex equations and, since $g(\zeta)$ has the value $-r^2$ for $\zeta = \epsilon_j$, setting $\zeta = \epsilon_j$ in (3.8) gives us N more. However, simply including these $2N$ extra equations in our set rather overdoes things, for we then have, in general, too many equations: they are not independent, and we must proceed with more care.

Our introduction of $g(\zeta)$ has led us to the conclusion that $f(\zeta)$ must have the structure exhibited in (3.17), but its sole purpose was to help us solve the nonlinear functional equation (2.7). The extra conditions we need can be obtained by substituting the form for $f(\zeta)$ in (3.17) into (2.7). Exploiting properties of the functions $F(z)$ and $G(z)$ given in Appendix A, we can write the result as

$$\prod_{j=1}^{N} \frac{F(\zeta/\epsilon_j)F(\overline{\epsilon}_j\zeta/q^2)}{F(\zeta/\gamma_j)F(\overline{\gamma}_j\zeta/q^2)} = q^{2-2N} \prod_{j=1}^{N} \overline{\gamma}_j\delta_j \frac{F(\zeta/\delta_j)F(\overline{\delta}_j\zeta/q^2)}{F(\zeta/\gamma_j)F(\overline{\gamma}_j\zeta/q^2)} + \frac{r^2}{E^2}. \tag{3.18}$$

Both sides of equation (3.18) are loxodromic functions, and the extra conditions needed are those ensuring that this is an *identity* between loxodromic functions.

We know from Appendix B that a loxodromic function is uniquely specified by

giving its zeros and poles, and its value at some other point. The functions on both sides of (3.18) obviously have the same poles. That on the left-hand side has zeros at $\zeta = \epsilon_j$ for $j = 1, 2, \ldots, N$, and that on the right-hand side has zeros at these points if and only if

$$q^{2-2N} \prod_{k=1}^{N} \overline{\gamma}_k \delta_k \frac{F(\epsilon_j/\delta_k) F(\overline{\delta}_k \epsilon_j/q^2)}{F(\epsilon_j/\gamma_k) F(\overline{\gamma}_k \epsilon_j/q^2)} = -\frac{r^2}{E^2} \qquad \text{for } j = 1, 2, \ldots, N. \tag{3.19}$$

That on the left-hand side also has zeros at $\zeta = q^2/\overline{\epsilon}_j$ for $j = 1, 2, \ldots, N$, but condition (3.19) already ensures that the right-hand side has these same zeros.

We need one further condition to ensure that (3.18) is an identity. The simplest form of this condition is obtained if we multiply through by the denominator of the products appearing in (3.18), and then set $\zeta = \gamma_1$. This is effectively equating residues at the simple pole $\zeta = \gamma_1$ on both sides of (3.18), rather than equating values at a regular point, to determine the multiplicative constant in the representation (B 9), and leads to

$$\prod_{k=1}^{N} F(\gamma_1/\epsilon_k) F(\overline{\epsilon}_k \gamma_1/q^2) = q^{2-2N} \prod_{k=1}^{N} \overline{\gamma}_k \delta_k F(\gamma_1/\delta_k) F(\overline{\delta}_k \gamma_1/q^2). \tag{3.20}$$

However, the loxodromic functions in (3.18) also enjoy the symmetry expressed by (B 10), so that the constant C in the representation (B 9) must be real and the only extra condition we need arises from the *real* part of (3.20)—unless we have exceptional circumstances with both sides of (3.20) purely imaginary. Then we can take the imaginary part of (3.20) instead; we could also equate the moduli of both sides. In fact, this detail caused no problems during any of the computations for the examples reported in § 5; the real part of (3.20) proved to be effective throughout.

One might think that one must also impose one or both of (3.9) and (3.11), but this is not so. If we do not have condition (B 8), then the representation for $l(z)$ in (B 9) gives a function that acquires a multiplicative factor when z is replaced by $q^2 z$; see (B 4). The form of (3.18) forbids such behaviour, and our solutions automatically satisfy (3.9) and (3.11).

Equations (2.5) involve the β_j defined in (2.4). With $f(\zeta)$ of the form (3.17), we can write β_j in terms of the parameters appearing explicitly in that formula, and thus express (2.5) as a condition with β_j absent. The result is considerably less elegant than (2.5) but, since it is the most convenient form of this restriction for computations, we record it as

$$E^2 \gamma_j \frac{F(\overline{\epsilon}_j \gamma_j) F(\epsilon_j/\gamma_j)}{F(\overline{\gamma}_j \gamma_j)} \frac{f'(\gamma_j)}{f(\gamma_j)} \prod_{\substack{k=1 \\ k \neq j}}^{N} \frac{F(\overline{\epsilon}_k \gamma_j) F(\epsilon_k/\gamma_j)}{F(\overline{\gamma}_k \gamma_j) F(\gamma_k/\gamma_j)}$$

$$= r_j^2 \prod_{n=1}^{\infty} (1 - q^{2n})^2 \qquad \text{for } j = 1, 2, \ldots, N; \tag{3.21}$$

the empty product that arises when $N = 1$ is to be interpreted as 1.

We note that the logarithmic derivative of $f(\zeta)$ appears in (3.21). Since $f(\zeta)$ is expressed in terms of F-functions and G-functions that are themselves defined as products, this can be written in a simple form that is easily evaluated.

4. Conditions in the air hole

We now consider the extra condition that arises from the assumption made concerning the physical properties of the air hole. We could simply specify its area; this is relevant when we consider injection of fluid and suppose that effectively incompressible air is trapped in the hole, or when we change the area of the hole by extracting or adding air. The most convenient formula for the area of the air hole for computational purposes is that obtained by subtracting the area occupied by fluid from the total area enclosed by the outer boundary of the blob. Using Green's theorem, we find that

$$\text{hole area} = \frac{1}{2\mathrm{i}} \int_{|\zeta|=1} \overline{f(1/\bar{\zeta})} f'(\zeta)\, \mathrm{d}\zeta - \pi r^2 - \pi \sum_{j=1}^{N} r_j^2, \tag{4.1}$$

where the integral is taken anti-clockwise round $|\zeta| = 1$.

The other assumption concerning the air hole we consider here is that relevant when the hole is provided with a suitably placed air vent. We then suppose that the same constant pressure acts on both the inner and outer boundaries of the blob. The mathematical implications of this in a general setting are discussed by Richardson (1994) and emerge when we consider the time-development of a functional of the domain $D = D(t)$ occupied by the blob that is formed by integrating over D a time-independent harmonic function whose harmonic conjugate in D is *multi-valued*: the evolution of the Cauchy transform itself, as given here by (1.3) and (1.4), follows from similar considerations using harmonic functions whose harmonic conjugate in D is *single-valued*. As long as the blob in the z-plane does not cover the origin $z = 0$, the natural such harmonic function to use is $\log|z|$, and manipulations analogous to those given in Richardson (1994) lead us to the condition

$$r^2 \log|f(\zeta_q)| + \tfrac{1}{2}\{|f(\zeta_q)|^2 - |f(\zeta_1)|^2\} - \mathrm{Re}\left\{ \int_{\zeta_1}^{\zeta_q} \overline{f(1/\bar{\zeta})} f'(\zeta)\, \mathrm{d}\zeta \right\} = \text{const.} \tag{4.2}$$

Here ζ_1 can be any point on $|\zeta| = 1$ and ζ_q any point on $|\zeta| = q$, and the path of integration from ζ_1 to ζ_q can be chosen arbitrarily within the annulus $q < |\zeta| < 1$ provided it avoids the singularities of the integrand there. It is easy to show that different choices of ζ_1, ζ_q and the path of integration do not affect condition (4.2), and it is useful to have this freedom. In a simple example with all the singularities of $f(\zeta)$ on the positive real axis, we can take $\zeta_1 = -1$ and $\zeta_q = -q$, and integrate along the negative real axis. In a slightly more complicated example with singularities on this portion of the negative real axis as well, this choice is not possible but we can then take $\zeta_1 = -\mathrm{i}$ and $\zeta_q = -\mathrm{i}q$ and integrate up the imaginary axis—provided there are no singularities on *this* path.

When the blob has moved to cover the origin $z = 0$, the approach suggested above using $\log|z|$ is not feasible and it seems we must begin again using, say, $\log|z - z_0|$ where z_0 is chosen as a new fixed point within the air hole. However, the special role played by the origin in its derivation has disappeared from (4.2) and the new approach must lead to the same condition; equation (4.2) is applicable throughout the motion.

If we begin injecting into an initial annulus of fluid centred on $z = 0$ with inner radius ρ_i and outer radius ρ_o, keeping pressures on the inner and outer boundaries

PHILOSOPHICAL TRANSACTIONS OF THE ROYAL SOCIETY A MATHEMATICAL, PHYSICAL & ENGINEERING SCIENCES

equal, we find that in (4.2) we need

$$\text{const.} = \rho_o^2 \left(\log \rho_o - \tfrac{1}{2}\right) - \rho_i^2 \left(\log \rho_i - \tfrac{1}{2}\right). \tag{4.3}$$

In fact, this value for the constant is also correct in circumstances where one might think otherwise. Suppose we have the annulus above, but begin injecting at a point either within the air hole in $|z| < \rho_i$ or in the outer region $|z| > \rho_o$, but still keep the pressures on all free boundaries (now three of them) the same. We initially have a circular blob growing about the injection point, but the annulus of fluid remains unaffected until this blob has grown to touch it. Subsequently, we have a doubly connected blob to which the present theory applies, but the initial state for this motion is a degenerate one with a circular annulus plus a circular disc that is tangential to it. Nevertheless, the resulting motion when we maintain equal pressures is subject to restriction (4.2) with the constant still given by (4.3). The mathematical form of (4.2) correctly reflects the physical assumption that the entire motion has evolved from an original annulus of fluid, with equal pressures being maintained on all the free boundaries involved throughout.

A number of other assumptions concerning the air hole may be contemplated. For example, we may impose a given pressure difference between the inner and outer boundaries, or suppose compressible air to be trapped in the hole so that some relation between the area of the air hole and the pressure within it is known. The necessary equations can be derived from the results in Richardson (1994). However, we here confine our attention to situations where either the area of the air hole varies in a known manner, when equation (4.1) is relevant, or where the same pressure is maintained on both free boundaries, when equation (4.2) is to be employed.

We now have all the equations we need to determine the plan-view of the basic annulus of area πr^2 after it has been subjected to injection of fluid of area πr_j^2 at each injection point $z = a_j$ for $j = 1, 2, \ldots, N$. It is given by the map $z = f(\zeta)$ of the annulus $q < |\zeta| < 1$, where $f(\zeta)$ has the form (3.17) involving the 2 real parameters E and q, and the $3N$ complex parameters γ_j, δ_j and ϵ_j. These are determined by solving the $3N$ complex equations (2.1), (3.19) and (3.21), the equation comprising the real part of (3.20), and whichever of the real equations (4.1) or (4.2) is appropriate. Whenever we have symmetry we can, of course, exploit this to simplify matters. For example, when $N = 1$ we would naturally take a_1 to be real; all the five parameters E, q, γ_1, δ_1 and ϵ_1 are then real, and the restrictions to be imposed reduce to a set of five real equations.

In the next section, we present examples solved by the method we have developed. The mathematical details are kept to a minimum so that we may concentrate on other features of interest; general comments concerning the computations needed when dealing with such problems appear in § 6.

5. Examples

The simplest examples of motions to which our analysis applies concern injection of fluid at just one point into an initial annulus of fluid. Figure 1 shows such a motion when we suppose the air pressures on both free boundaries to be equal. In all the figures, the centre of the basic annulus and the relevant injection (or suction) points are marked by dots, as are points where an air hole vanishes. No axes are drawn but, as in the analysis, the origin of our Cartesian coordinate system is at the centre of the basic annulus, and the coordinates of other points are given supposing the usual

PHILOSOPHICAL TRANSACTIONS OF THE ROYAL SOCIETY A MATHEMATICAL, PHYSICAL & ENGINEERING SCIENCES

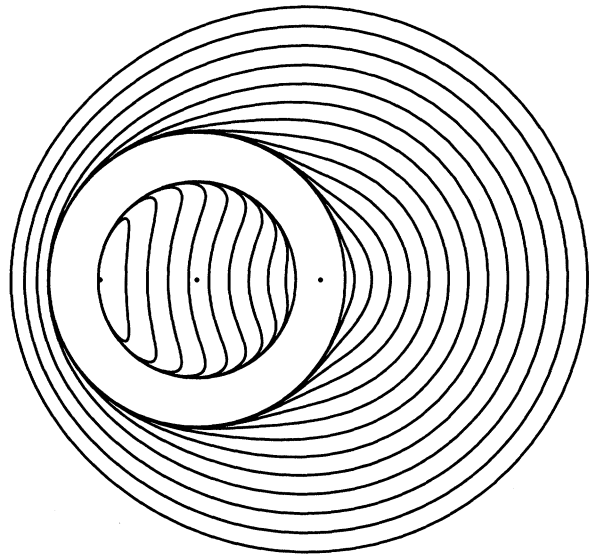

Figure 1. Injection into an initial annulus of inner radius 2 and outer radius 3 at the point $(2.5, 0)$ when the pressures on both free boundaries are kept the same. After injecting an area 16.13π, the hole disappears at the point $(-1.960, 0)$. With πr_1^2 the area injected, the blob outline is drawn for 10 equal increments in r_1 as πr_1^2 increases from 0 to 16.13π. Three further outlines are drawn as the blob continues to expand as a simply connected region after the air hole has vanished, the same increments in r_1 being used for these.

orientation with the x-axis to the right and the y-axis vertically upwards. Numerical values given to 4 figures are correctly rounded to 4 significant figures; those given to fewer than 4 figures are exact.

In figure 1, the initial annulus has an inner radius of 2 and an outer radius of 3, and injection takes place at $(2.5, 0)$. The air hole disappears at the point $(-1.960, 0)$ after an area 16.13π has been injected.

The early stages of the motion shown in figure 1 simply involve a bulging of the annulus around the injection point, there being very little movement elsewhere. Indeed, we are tempted to use the terminology of optics: with a point source of light at the injection point, the air hole casts a shadow within which very little happens. In fact, the fluid motion is driven by a pressure field that is harmonic, which has a logarithmic singularity at the injection point, and which we may suppose to be zero on both free boundaries, and this pressure is exponentially small in the shadow. A consequence of this is that the point where the air hole vanishes is very close to the inner boundary of the initial annulus. If this motion is to model injection into a Hele-Shaw cell with an air vent provided to ensure the necessary equality of pressures, it is at the point $(-1.960, 0)$ that the air vent must be placed.

What happens if we begin with an annulus of fluid as in figure 1, still keep the pressures on the inner and outer boundaries equal, but apply *suction* at a point within the fluid instead of *injection*? Some familiarity with similar scenarios leads one to expect that a cusp will appear, and that it will appear in the inner free boundary if the suction point is close to the inner boundary, but in the outer free boundary if the suction point is close to the outer boundary—and, presumably, a cusp will appear simultaneously in both boundaries if the suction point is positioned at some point

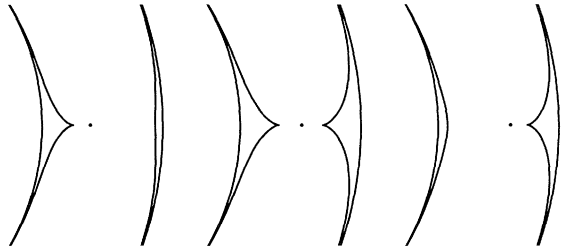

Figure 2. Three cases with suction from the initial annulus of inner radius 2 and outer radius 3, so that the initial hole area is $4\pi = 12.57$, when the pressures on both free boundaries are kept the same. Only the region in $-1 < y < +1$ near the suction point is drawn, and the curves show the initial annulus, together with the blob outline at the instant cusps appear. From left to right, the suction point is at $(2.4, 0)$, $(2.511, 0)$ and $(2.6, 0)$, the cusps appear when the area of fluid withdrawn is 0.05557π, 0.1006π and 0.06138π and the area of the air hole is 12.67, 12.71 and 12.63, and the inner boundary then crosses the x-axis at $x = 2.259$, 2.321 and 2.078 while the outer boundary crosses it at $x = 2.937$, 2.685 and 2.738. The last two lists of numbers give the location of the cusp when the relevant boundary is cusped. In the middle sketch, there are cusps in both boundaries.

in between. That this is indeed what happens is seen in figure 2 where we have the same initial annulus with inner radius 2 and outer radius 3 as in figure 1, and show the effect of suction at three different points; since there is little motion elsewhere, only a small region near the suction point is drawn in each case. The advent of cusps in such situations signals a breakdown: there is no acceptable solution of our equations if we try to suck out further fluid. The cusps appear simultaneously in both free boundaries when we apply suction at $(2.511, 0)$, this being the situation in the middle sketch of figure 2.

Starting with the same annulus as in figure 1 and maintaining equal pressures on both boundaries, we may contemplate injecting at a point that is not initially covered by fluid. To begin with, we then have just an expanding circular blob with the annulus not affected until this growing blob touches it. The situation when the injection is outside the annulus at $(4, 0)$ is illustrated in figure 3. The air hole now disappears at the point $(-1.953, 0)$ after a total area of 29.10π has been injected. When the injection is inside the original air hole at $(1, 0)$, we have the motion in figure 4. The air hole now disappears at the point $(-1.975, 0)$ after a total area of 7.513π has been injected. Note that the sequence of figures 3, 1, and then 4 has the injection point moving successively to the left, and the point where the air hole vanishes moves to the left too. If we inject at the origin, the growing circular disc obviously hits all points on the inner boundary of the annulus simultaneously but, thought of as the limit of the sequence envisaged above, this scenario has its vanishing point at $(-2, 0)$.

What happens if we begin injecting as in figure 1, but suppose the area of the air hole to remain constant? At first, we still expect the principal effect to be the growth of a bulge in the annulus near the injection point but, to stop the area of the hole from decreasing as it does in figure 1, the pressure within the hole must now be greater than that outside. This means that the portion of the annulus away from the injection point is subjected to a radial pressure gradient and will tend to move outwards, thinning as it does so to conserve area. The configuration that such arguments suggest would eventually evolve has a large, almost-circular blob with a

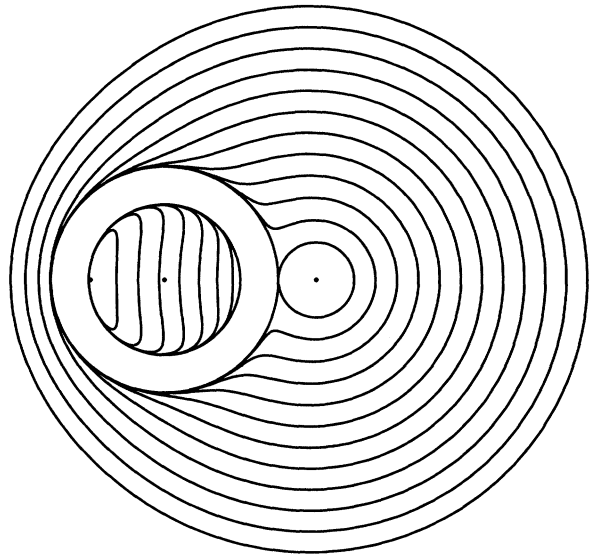

Figure 3. Injection at the point $(4, 0)$ with an initial annulus of inner radius 2 and outer radius 3 when the pressures on both free boundaries are kept the same. After injecting a total area 29.10π, the hole disappears at the point $(-1.953, 0)$. With πr_1^2 the area injected, the blob outline is drawn for 8 equal increments in r_1 as πr_1^2 increases from π to 29.10π. Three further outlines are drawn as the blob continues to expand as a simply connected region after the air hole has vanished, the same increments in r_1 being used for these.

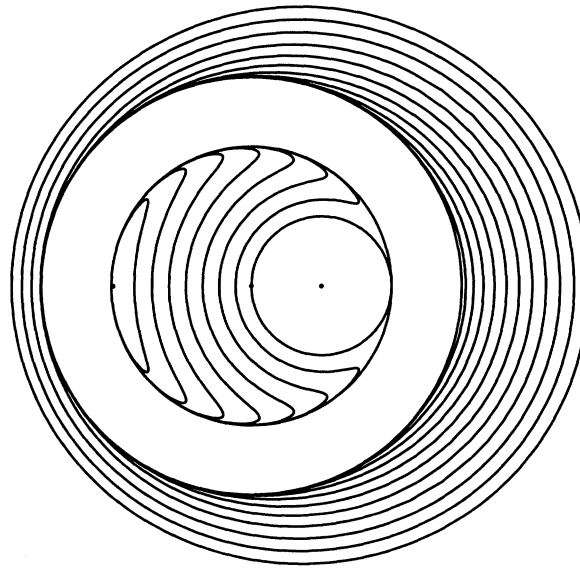

Figure 4. Injection at the point $(1, 0)$ with an initial annulus of inner radius 2 and outer radius 3 when the pressures on both free boundaries are kept the same. After injecting a total area 7.513π, the hole disappears at the point $(-1.975, 0)$. Plotting details are as for figure 3, with one obvious numerical change.

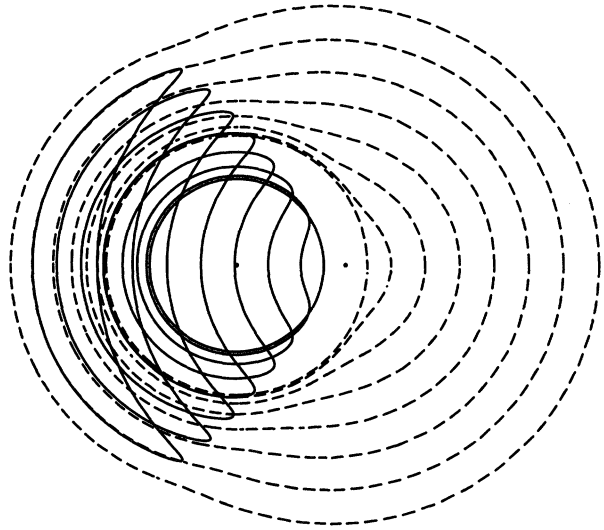

Figure 5. Injection at the point $(2.5, 0)$ with an initial annulus of inner radius 2 and outer radius 3, the area of the air hole being kept constant at the value 4π. Inner boundary curves are shown solid, while the outer ones are dashed. With πr_1^2 the area injected, the curves are drawn at increments of 0.8 in r_1 from 0 to 5.6.

thin annular arc joined to it on the left; the hole has become almost crescent-shaped with a boundary that has two short sections of very large curvature where the annular arc joins the almost-circular blob and, while one portion of the inner boundary between these two sections of large curvature is moving so that fluid advances *towards* the air, the other has the fluid retreating *from* the air. Conventional wisdom seems to suggest that such a solution is unlikely to persist and would break down, perhaps by the formation of cusps where the curvature is already high. However, no such breakdown was encountered during the computations, and the solution does indeed appear to continue as conjectured above for ever. The motion is illustrated in figure 5.

We now have a more complicated picture than in previous examples, for the inner boundary traverses regions that were earlier crossed by the outer boundary. In figure 5, we have tried to clarify the situation by drawing the outer boundaries dashed. The same blob outlines are drawn in sequence in figure 6 which, perhaps, gives a clearer impression of the entire motion. However, some details that are evident in figure 5 are no longer so obvious in figure 6. For example, we can see in figure 5 that the annular arc on the left really does expand as if it were part of a complete expanding annulus, and one needs the curves to be superposed to see this. In similar future examples, we present the results either in the superposed form of figure 5, or in the array format of figure 6, using the latter when the former is deemed to be too confusing.

The contention that this motion with the area of the air hole maintained constant leads to no breakdown is supported by a further observation: the extreme configurations towards which the sequence in figure 6 is tending can be reached by a different route that is reminiscent of the motion in figure 4. Both figure 4 and figure 6 begin with a basic annulus of inner radius 2 and outer radius 3, so that the annulus has

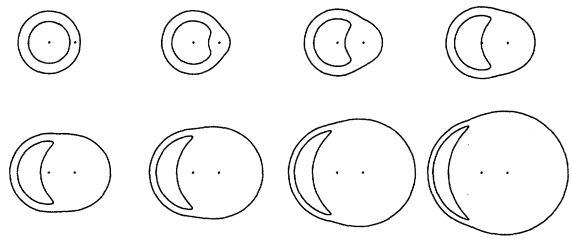

Figure 6. The same motion and curves as in figure 5, but now presented in a time-sequence from top-left to bottom-right.

area 5π and the hole has area 4π. Increase the pressure inside this annulus so that it grows until it has a large radius and is very thin, but still has area 5π. Now inject at the point $(2.5, 0)$ used in figure 6, but do so with the pressures on all boundaries kept at the same constant value. A circular disc grows about $(2.5, 0)$ and eventually touches the large, thin annulus internally; at this instant, the area of the air hole is *greater* than 4π, the area of the hole in figure 6. Further injection with equal pressures on all free boundaries produces a motion qualitatively as in figure 4, with the area of the air hole decreasing—and as this area decreases through the value 4π, we have arrived at a configuration that belongs in the sequence of figure 6.

What happens if we begin as in figures 5 and 6, still keep the area of the hole constant, but apply *suction* instead of *injection*? We expect the situation to be qualitatively as illustrated in figure 2, except that the major part of the annulus will move inwards a very small distance before the solutions break down when the cusps appear. This is indeed the case, and if we start with the same annulus of inner radius 2 and outer radius 3, the quantitative changes produced by the different conditions yield a picture that is barely distinguishable from that in figure 2 and we do not, therefore, reproduce it. There is some interest in noting the quantitative changes. For example, the suction point in figure 2 is at $(2.511, 0)$ to produce cusps simultaneously in both boundaries, but with the area of the hole kept constant it needs to be at $(2.502, 0)$. If we did reproduce a figure analogous to figure 2 for this case, its caption would record that, from left to right, the suction point is at $(2.4, 0)$, $(2.502, 0)$ and $(2.6, 0)$, the cusps appear when the area of fluid withdrawn is 0.05812π, 0.1014π and 0.06021π, and the inner boundary then crosses the x-axis at $x = 2.255$, 2.311 and 2.070 while the outer boundary crosses it at $x = 2.926$, 2.676 and 2.737.

If we begin with the geometry and injection point as in figure 3 but keep the hole area constant, we obtain the result in figure 7. As in figures 5 and 6, the plan-view approaches that of an almost-circular blob with a thin annular arc attached, and again the numerical work suggests that the breakdown one might expect does not occur. Once more, the extreme configurations towards which those shown in figure 7 are tending can be reached by a different route.

What if we begin with the geometry and injection point as in figure 4, but keep the hole area constant? There are, in fact, two possible interpretations for this question. If we begin injecting at $(1, 0)$ into a hole containing incompressible air, the annulus must grow as the circular blob itself grows, but the growing circular blob does eventually touch the inner boundary of the annulus when the radius of the circular blob is 1.5 and the inner radius of the annulus is 2.5, if the starting dimensions are as in figure 4. Alternatively, we may wish to consider the initial configuration to be that

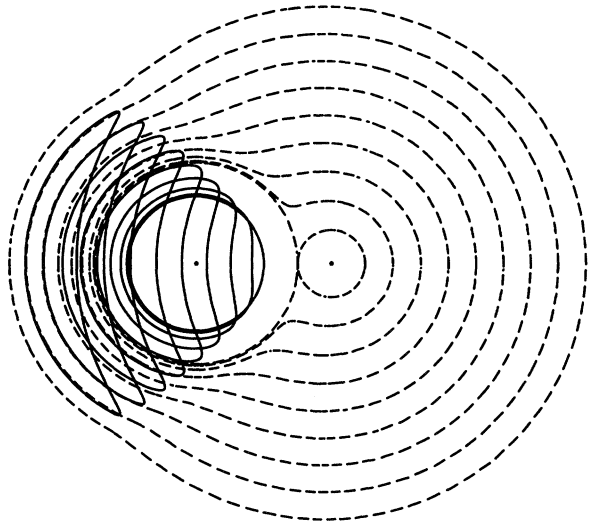

Figure 7. Injection at the point $(4, 0)$ with an initial annulus of inner radius 2 and outer radius 3 when the hole area is kept constant at the value 4π. Inner boundary curves are shown solid, while the outer ones are dashed. With πr_1^2 the area injected, the curves are drawn at increments of 0.8 in r_1 from 1 to 7.4.

in figure 4, with a circular disc of radius 1 centred on $(1, 0)$ already touching the annulus of inner radius 2. Whichever interpretation we choose, *there is no solution within the confines of our model beyond the instant when the circular disc touches the annulus*. The difficulty is precisely the same as that encountered in Richardson (1994) when considering injection near a corner with incompressible air trapped in the corner, and we may make similar observations. In particular, if there *were* a solution with a constant hole area beyond the instant of touching, it would be attainable by a different route. To be specific, consider the second of the two interpretations mentioned above, so that the hole has area 3π and we are beginning with the configuration comprising the disc and annulus shown in figure 4. Injecting with equal pressures for a short while, we reach another configuration shown in figure 4, but the hole area has decreased below 3π. Stop the injection of fluid, and now try to increase the hole area back up to the value 3π by increasing the air pressure. We find that cusps appear (in the obvious places) to thwart our attempt. The situation is, in all qualitative respects, identical with that discussed in greater detail by Richardson (1994).

Suppose, now, we inject just a small amount of fluid at a point into an annulus; whether this is done under the equal-pressures constraint of figure 1 or the constant-hole-area constraint of figure 5 is not relevant, for we merely wish to consider the resulting annulus-with-a-bulge as the starting configuration for further motion. What happens if we now increase the area of the hole? In fact, the expansion results in a circular disc centred on the original injection point and containing exactly the same area of fluid as was originally injected being left behind by an expanding annulus. If we decrease the area of the hole instead then, provided the initial dimensions are suitably chosen (see below), a circular disc of fluid of exactly the same size and in

PHILOSOPHICAL TRANSACTIONS OF THE ROYAL SOCIETY A MATHEMATICAL, PHYSICAL & ENGINEERING SCIENCES

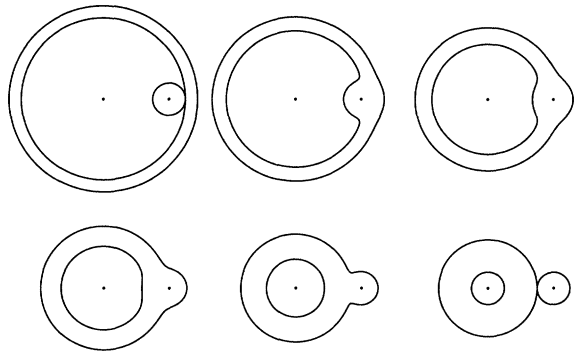

Figure 8. A shrinking annulus of fluid of area 8π absorbs and disgorges a circular disc of fluid of radius 1 with centre at $(4, 0)$. When touching as at top-left, the inner and outer radii of the annulus are 5 and $\sqrt{33}$, and the area of the hole is 24π. When touching as at bottom-right, the inner and outer radii are 1 and 3, and the area of the hole is π. With πR^2 the area of the hole in a general position, the sketches are drawn for equal decrements of R from $\sqrt{24}$ down to 1.

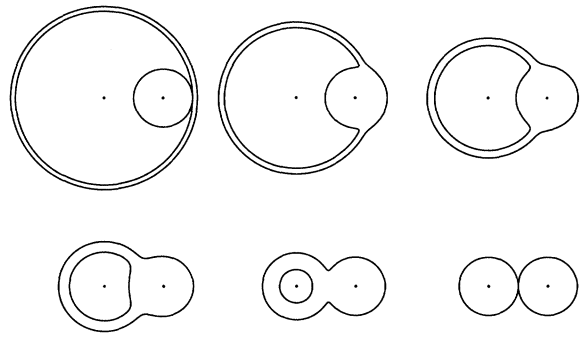

Figure 9. A shrinking annulus of fluid of area π absorbs a circular disc of fluid of radius 1 with centre at $(2, 0)$, the final state now consisting of two touching circular discs of radius 1; the hole vanishes at the origin. In the sketch at top-left, the inner and outer radii of the annulus are 3 and $\sqrt{10}$, and the area of the hole is 8π. With πR^2 the area of the hole in a general position, the sketches are drawn for equal decrements of R from $\sqrt{8}$ down to 0.

exactly the same position as above is left behind by a shrinking annulus. The entire sequence models the interaction that occurs as an annulus of fluid shrinks, absorbing and disgorging a circular disc of fluid as it does so. We have the annular analogue of the soliton-like behaviour noted by Richardson (1996*b*) in a different context. A particular example is illustrated in figure 8. The sequence here can, of course, be run in the opposite direction, so that an *expanding* annulus of fluid is involved.

With πr^2 the area of the annulus, and the circular disc of radius r_1 and centre $(a_1, 0)$, we obtain the scenario of figure 8 only if $r + r_1 < a_1$. With equality here instead of inequality, the hole vanishes at the instant the annulus is about to pull away from the disc, and the final configuration consists of two tangential circular discs. Figure 9 illustrates the motion when these final discs have equal radii.

We may interpret the sequence in figure 9 a little differently. We begin with a blob of fluid containing an air hole (and we may 'begin' anywhere along the sequence, not necessarily at top-left) and remove air from the hole; we successfully extract all the air, and the air hole disappears at the origin. Such an interpretation seems more

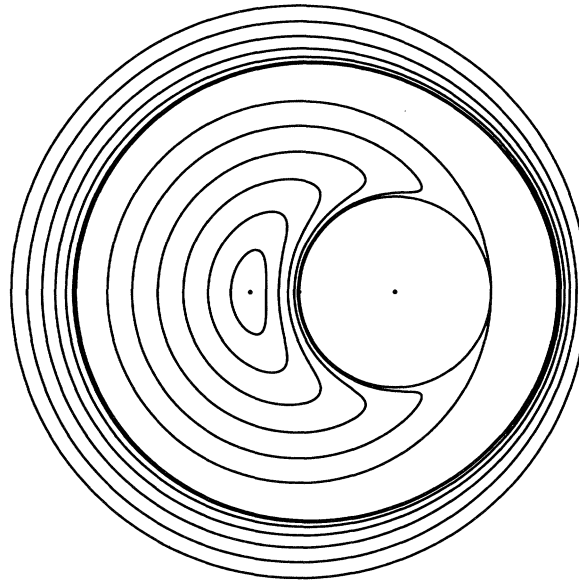

Figure 10. We begin with a fluid annulus of inner radius 2 and outer radius 3, and a circular fluid blob of radius 1 centred on $(1,0)$ that touches the annulus at $(2,0)$. Air is removed from the hole, and the air hole disappears at the point $(-0.5103,0)$. The initial area of the hole is 3π; with πR^2 equal to this area in general, the outline is drawn for 6 equal decrements in R from $\sqrt{3}$ down to 0.

natural when we consider a situation with the above inequality reversed, so we may suppose $0 < a_1 < r + r_1$. Figure 10 shows an instance with $a_1 = 1$, $r = \sqrt{5}$ and $r_1 = 1$.

In fact, the starting configuration in figure 10 is precisely the 'touching' configuration that served as a start for figure 4. We have an annulus with inner radius 2 and outer radius 3, and a circular disc of radius 1 centred at $(1,0)$, but we now have no injection of fluid and simply remove air from the hole. We are able to remove all the air successfully, but the position of the point where the hole vanishes cannot now be inferred so readily as it could in figure 9; it is at $(-0.5103,0)$. We consider how such vanishing points may be determined in § 7; we do not need to follow the intervening motion to find them. Remember, too, that any of the intermediate configurations appearing in figure 10 can be regarded as the starting configuration for further motion, these being rather less extreme shapes than the annulus-plus-disc that our presentation labels as the beginning.

When discussing figure 1, involving injection with pressures kept equal on both boundaries, we noted that there was little movement in the region that would be occupied by the shadow cast by the air hole with a light source at the injection point. Conversely, the precise geometry of the region occupied by fluid in this shadow will have little effect on the motion in the illuminated region. Thus, if we were to produce a preliminary bulge in the annulus on the left by injection on the left, we expect that subsequent injection on the right, as in figure 1, would lead to a situation where the air hole is split into two. An example of this appears in figure 11. With the air hole thus divided, the region occupied by fluid is now *triply* connected, and the analysis presented in the present paper is not able to follow the motion any further.

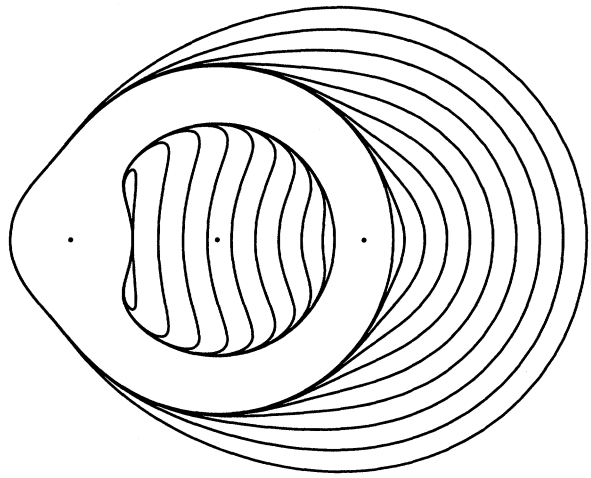

Figure 11. The initial configuration is formed by injecting an area $\pi(0.8)^2$ at $(-2.5, 0)$ into a basic annulus with inner radius 2 and outer radius 3, while equal pressures are maintained on the two free boundaries; this reduces the original hole area of $4\pi = 12.57$ to 11.71. Injection then proceeds at $(2.5, 0)$, still with pressures kept equal, and after injecting an area 13.08π here, the air hole divides into two as the inner boundary touches itself at the point $(-1.441, 0)$; the initial inner boundary passes through $(-1.442, 0)$. The *total* area of the air hole when touching occurs is 0.2549. With πr_1^2 the area injected at $(2.5, 0)$, the blob outline is drawn for 9 equal increments in r_1 as πr_1^2 increases from 0 to 13.08π.

What if we begin as in figure 11 with an annulus that has a bulge on the left, inject on the right as in figure 11, but now keep the hole area constant? Figures 5 and 6 might suggest that an annular-arc-plus-bulge moves to the left, but this cannot be correct. (Both $h_e(z)$ and $h_1(z)$ in (1.7) have a singularity at the preliminary injection point on the left, and this point must remain covered by fluid.) A correct inference can be drawn from a time-reversal of figure 8: an annular arc *does* move to the left, but leaves behind a circular disc centred on the preliminary injection point that contains an area equal to that inserted during this preparatory injection—and then this circular disc is absorbed into the expanding almost-circular portion of the blob that is growing about the new injection point. The sequence of configurations through which the plan-view passes is shown in figure 12.

Some further comments seem to be called for. If the preliminary bulge on the left had been only a little larger, the emerging circular disc would obviously be too large to fit in the hole; as with figure 11, we would progress to a fluid region that is triply connected and a different theory would be needed to follow the motion further. The ideas in figures 8 and 12 can also be combined with those in earlier examples. If a small isolated circular blob were to the left in figures 5, 6 or 7, it would first be absorbed into the advancing annular arc and then disgorged from it into the hole, before being reabsorbed into the almost-circular portion on the right—unless the isolated blob was too large and led to triply connected difficulties. An isolated circular blob to the right in figures 5, 6 or 7 would, of course, simply be absorbed directly into the main almost-circular portion.

In figure 13, we begin with an annulus of fluid of inner radius 2 and outer radius 3, plus two circular discs of fluid, one of radius 0.95 and the other of radius 0.78. The

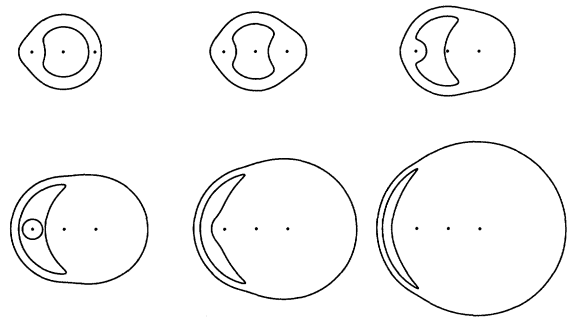

Figure 12. The initial configuration is as in figure 11, and injection is still at $(2.5, 0)$, but the area of the air hole is maintained at the value 11.71 instead of keeping the pressures equal. With πr_1^2 the area injected at $(2.5, 0)$, the outlines are drawn for equal increments of 1.3 in r_1 from 0 to 6.5. The disc of radius 0.8 centred on $(-2.5, 0)$ is disgorged when $r_1 = 3.441$ and reabsorbed when $r_1 = 4.111$.

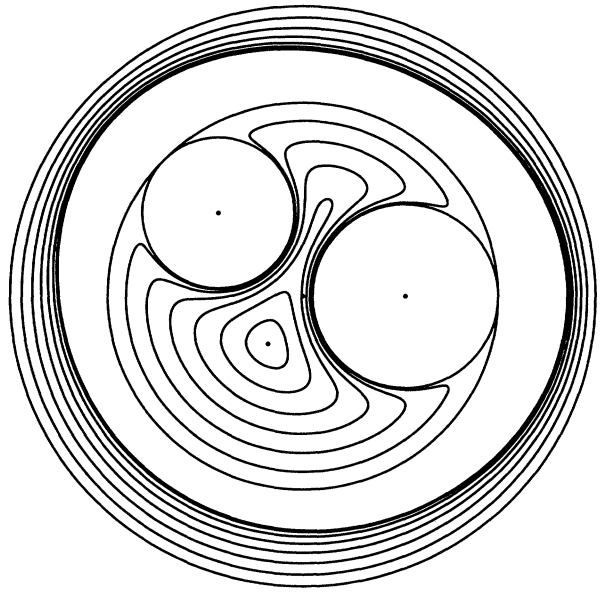

Figure 13. We begin with an annulus of fluid of inner radius 2 and outer radius 3, plus two circular discs of fluid that just touch the annulus. One disc is of radius 0.95 with its centre on the x-axis and the other is of radius 0.78 with its centre on the bisector of the axes in the second quadrant. The motion is driven by removing air from the air hole, which disappears at the point $(-0.3562, -0.4945)$. The initial area of the hole is 7.820. With πR^2 the hole area in general, the blob outline is drawn for seven equal decrements in R as πR^2 decreases from 7.820 to 0.

former has its centre on the x-axis, while the latter has its centre on the bisector of the axes in the second quadrant, and both are positioned so as to touch the inner boundary of the annulus. The motion is driven simply by removing the air, and we see that it can all be successfully extracted; the air hole vanishes at the point $(-0.3562, -0.4945)$. However, we also see that a tongue of air protruding to the top-right almost doesn't make it, and one feels that with slightly altered geometric parameters, the outcome could be rather different.

In figure 14, just one change has been made to the initial state in figure 13. The circular disc at top-left now has the larger radius of 0.85; its centre is still in the

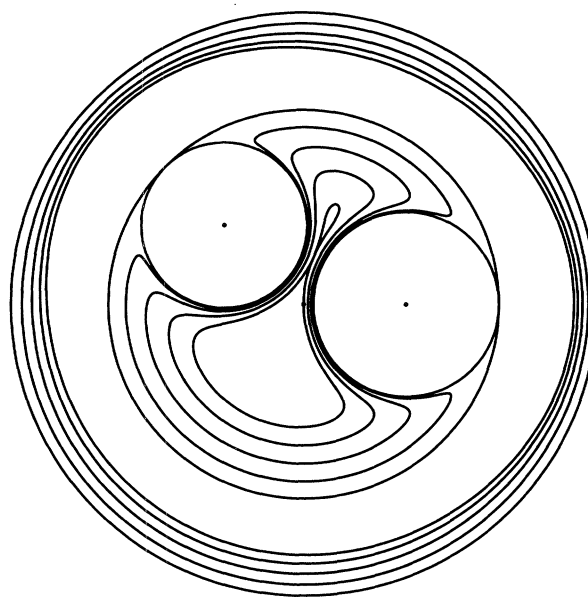

Figure 14. The starting configuration is as in figure 13, except that the upper-left disc has the larger radius 0.85. The hole area initially is 7.461, and when it has been reduced to 1.378 the boundary of the air hole touches itself at the point $(0.1034, 0.4893)$, dividing the hole into a lower-left lobe of area 1.346 and an upper-right lobe of area 0.03142. With πR^2 the hole area, the blob outline is drawn for four equal decrements of R as πR^2 decreases from 7.461 to 1.378.

second quadrant on the bisector of the axes, positioned so that the disc just touches the annulus. Now we see that the removal of air causes the air hole to be split into two. The fluid region then becomes triply connected, and a different solution scheme is necessary to follow the subsequent motion. If we were extracting the air at a point within the lower-left lobe, we could presumably continue extracting air from that portion, but the air in the smaller upper-right lobe would be irretrievable by this means. Similarly, extraction from within the upper-right lobe would leave the air in the larger lower-left lobe behind.

An interesting situation arises on the borderline between the two types of behaviour illustrated in figures 13 and 14. If we begin with the initial geometry as in figure 14, and then consider slightly different starting configurations with the upper-left disc having successively smaller radii, we must eventually reach a radius where the air hole no longer splits into two and all the air *can* be extracted with the hole remaining connected. Examining figures 13 and 14, it is not difficult to see that the boundary of the air hole must pass through a cusped state in this borderline situation; both before and after this cusped state, the boundary is smooth. The situation is quite different from that illustrated in figure 2 where the advent of the cusps signals a breakdown of the solution. That motions involving free boundaries in Hele-Shaw flows can pass *through* cusped states was observed by Howison (1986), and he also noted that such cusps must have a quite different structure from those that result in breakdown. Here, it is necessary to appreciate this different structure in order to compute the radius of the upper-left disc needed to obtain this cusped configuration; details are given in § 8.

To obtain the cusp, the radius of the upper-left disc must be 0.8150, and the

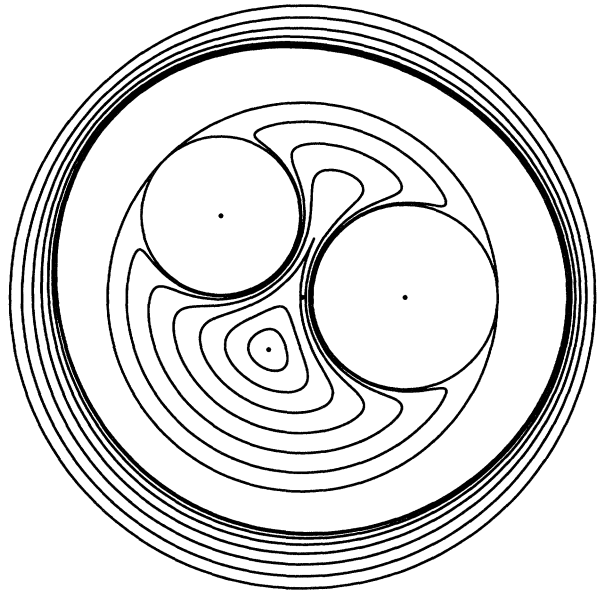

Figure 15. The starting configuration is as in figures 13 and 14, except that the upper-left disc now has radius 0.8150. The hole area initially is 7.644, and when it has been reduced to 1.178 a cusp appears in the boundary of the hole at the point $(0.1197, 0.6026)$. Nevertheless, the motion continues so that all the air can be extracted, with the air hole remaining connected and disappearing at the point $(-0.3456, -0.5405)$. With πR^2 the hole area, the blob outline is drawn for four equal decrements of R as πR^2 decreases from 7.644 to 1.178, and for 3 further equal decrements of R as πR^2 decreases from 1.178 to 0. Thus the cusped outline of the air hole appears in the figure.

resultant motion is sketched in figure 15. All the air can be removed, and the air hole vanishes at the point $(-0.3456, -0.5405)$.

In fact, exploiting the idea behind the topological changes that feature in figures 13, 14 and 15, one can devise other scenarios where a careful choice of geometrical parameters leads to motions that pass through cusped configurations, and the settings need not be as complicated as those considered in this paper. In particular, one can arrange for them to appear in simple motions arising from injection into an empty cell at a finite number of points, when the conformal maps involved are given by rational functions (Richardson 1996*a*), or in motions along infinite strips, when the conformal maps are given by functions whose derivative is elliptic (Richardson 1996*b*). To be specific, suppose we have two disjoint circular discs of fluid, and let them be hit simultaneously by an advancing straight or circular free boundary. If the discs are far apart, they are absorbed into the advancing boundary with no difficulty but, if they are sufficiently close together, an air pocket becomes trapped. With their separation carefully chosen between these two extremes, we pass through a cusped configuration. Naturally, perturbations of this same idea produce the same effect: the initial disjoint regions of fluid need not be circular, the advancing free boundary need be neither straight nor circular, and the initial blobs need not be hit simultaneously.

Such a cusp can also be produced by perturbing one of our earlier examples. Suppose that in figure 11 we move the initial bulge round the annulus, say in the clockwise sense, but keep everything else the same. Moving it through only a small angle, we still have the same qualitative picture as in figure 11 with the air hole

dividing into two parts. But if we move it somewhat further—certainly if we take it to the 12 o'clock position—the air hole contracts past the bump while remaining connected, and continued injection results in the hole vanishing at a single point. With a bulge in some intermediate position between these two extremes, the inner boundary of the blob again passes through a cusped state.

A different proposal for constructing motions that pass through cusped configurations has been presented by Hohlov & Howison (1993).

6. Computational concerns

All the computations required for this paper were performed by exploiting a path-following algorithm. No matter what the actual starting point may be in an example, the computations always began with the basic annulus. The arguments needed to explain the approach are similar to those used to deduce that we must have $n = 1$ in (3.16), an essential part of our derivation of the final form obtained for $f(\zeta)$ in (3.17).

With ρ_i the inner radius of the basic annulus in the z-plane and ρ_o its outer radius, the annulus $q < |\zeta| < 1$ in the ζ-plane onto which it is mapped conformally by $z = f(\zeta)$ has $q = \rho_\mathrm{i}/\rho_\mathrm{o}$. Suppose that we have the simplest case $N = 1$ and place the injection (or suction) point $z = a_1$ on the positive real axis. We are to be injecting directly into the fluid region (or sucking from it) so that $\rho_\mathrm{i} < a_1 < \rho_\mathrm{o}$; this computational starting point is the *actual* starting point for figures 1, 2, 5 and 6, but not for any of the other figures.

The relevant degenerate form of the map (3.17) is $f(\zeta) = \rho_\mathrm{o}\,\zeta$ and the image of the injection point in the ζ-plane is at $\zeta = \gamma_1 = a_1/\rho_\mathrm{o}$. Since the degeneration has $\delta_1 = \epsilon_1 = q^2/\gamma_1$, this initial state corresponds to

$$E = \rho_\mathrm{o}, \quad q = \frac{\rho_\mathrm{i}}{\rho_\mathrm{o}}, \quad \gamma_1 = \frac{a_1}{\rho_\mathrm{o}}, \quad \delta_1 = \epsilon_1 = \frac{\rho_\mathrm{i}^2}{\rho_\mathrm{o} a_1}. \tag{6.1}$$

With a_1 real and positive, all five parameters E, q, γ_1, δ_1 and ϵ_1 to be solved for are also real and positive, and we have five real equations (2.1), (3.19), (3.20), (3.21), and whichever of (4.1) and (4.2) is appropriate. These are solved by iteration, but we need sufficiently accurate estimates for the solution to begin the process. With only a small amount of injection (or suction) at $z = a_1$, we know the solution must yield values close to those in (6.1), but these correspond to a degenerate situation with a wholesale cancellation of zeros and poles; our estimates have to ensure that these zeros and poles are separated in the correct manner. If we really do have *injection* at $z = a_1$, so that $r_1^2 > 0$, then (2.5) implies that $\beta_1 > 0$ (initially $f'(\zeta) = \rho_\mathrm{o}$ for all ζ) and the pole of $g(\zeta)$ at $\zeta = \gamma_1$ has a positive residue; see equation (3.2). A consideration of the behaviour of $g(\zeta)$ along the ξ-axis, where it is real, shows that we must have

$$q^2/\gamma_1 < \epsilon_1 < \delta_1 \qquad \text{if } r_1^2 > 0: \tag{6.2}$$

recall that $g(\zeta)$ vanishes for $\zeta = \delta_1$ and $\zeta = q^2/\delta_1$, while it has the value $-r^2$ for $\zeta = \epsilon_1$ and $\zeta = q^2/\epsilon_1$. If we actually have *suction* at $z = a_1$, then $\beta_1 < 0$ and a similar argument shows that

$$\delta_1 < \epsilon_1 < q^2/\gamma_1 \qquad \text{if } r_1^2 < 0. \tag{6.3}$$

With a small amount of injection or suction, using estimates close to (6.1) that

respect either (6.2) or (6.3) as appropriate, we easily obtain the required solution. As the injection or suction is increased, we obtain sufficiently accurate estimates to find the solution by extrapolating earlier results.

The computations for figures 3 and 4 can exploit values obtained for figure 1. Take a solution for figure 1 that has r_1^2 somewhat greater than 1 (note that $r_1^2 = 1$ when the disc just touches the annulus in figures 3 and 4), but not so much greater that we run the risk of the air hole disappearing, and then follow a path that increases a_1 from 2.5 to 4 for figure 3, or decreases it from 2.5 to 1 for figure 4. This yields an intermediate curve for the appropriate figure, and subsequent decreases and increases of r_1^2 yield the remaining curves. It is interesting that this mathematical path-following procedure of changing a_1 with r_1^2 fixed, using equations (2.1), (3.19), (3.20), (3.21) and (4.2) throughout for figures 1, 3 and 4, has a physical counterpart. To move the physical system from a state obtained by injecting at one point to the state that would have been obtained had the injection been at a neighbouring point throughout, we inject at the second point while sucking at the first. By thus adjusting a_1 and r_1^2, we can move between any of the doubly connected configurations in figures 1, 3 and 4, keeping pressures on both free boundaries equal as we do so. This makes the mathematical result stated after equation (4.3) self-evident from a physical point of view: the constant that is needed in equation (4.2) when considering the motions in figures 3 and 4 is the one in (4.3) used for figure 1.

In the circumstances of figure 8, we can direct the initial calculations towards an intermediate stage in the sequence shown. Choose a q so that the basic annulus used covers the point $(4, 0)$ that is the centre of the disc involved. We can then solve the four real equations (2.1), (3.19), (3.20) and (3.21) for the four real parameters E, γ_1, δ_1 and ϵ_1 as r_1^2 increases from 0 to 1, with q fixed at this value. The result is a configuration that belongs in the sequence of figure 8, and we can use (4.1) to determine the corresponding hole area. Then path-follow while increasing and decreasing this hole area to progress towards the initial and final states in figure 8. A similar approach can be used in figure 9.

If we have a single injection point but choose not to site it on the positive real axis, the effect is simply to rotate the ζ-plane: the parameters E and q are not affected, but γ_1, δ_1 and ϵ_1 acquire a multiplicative factor of unit modulus that places them on some radial line other than the positive real axis. If we have several injection points round the annulus, the initial effect at each is largely independent of the presence of the others, and this fact allows one to obtain sufficiently accurate estimates to start a path-following routine with any number of injection points strictly within the initial basic annulus. If injection points that cannot be covered by the basic annulus are needed, these can be moved as above—or we can begin with a fatter annulus that *does* cover them, and path-follow as we make it thinner.

Using the ideas discussed thus far in this section, one can compute results for any motion of the type we are considering, but an alternative approach to the last two sketches in figure 12 seems worth mentioning for the light it sheds on the structure of the solutions. We here have $N = 2$, with injection at $z = a_1 = 2.5$ and $z = a_2 = -2.5$, so that all parameters are real, and we can reach these configurations by first injecting at $z = a_1$ a sufficient area πr_1^2 to cover the injection point at $z = a_2$, starting from the basic annulus. This is a calculation with $N = 1$ like that required for figures 5 and 6 except that we need a hole area of 11.71 instead of $4\pi = 12.57$, and we find values for E, q, γ_1, δ_1 and ϵ_1 that yield a corresponding map $z = f(\zeta)$. We now contemplate injecting at $z = a_2$, so we increase N to 2; as when injecting into the basic annulus,

PHILOSOPHICAL TRANSACTIONS OF THE ROYAL SOCIETY A MATHEMATICAL, PHYSICAL & ENGINEERING SCIENCES

zeros and poles move away from coalescence as this new injection point is born. At this birth, the relevant value of γ_2 is given by solving $f(\gamma_2) = a_2$ with the $f(\zeta)$ found above, and the coalescence of zeros and poles implies that we can then suppose that $\delta_2 = \epsilon_2 = q^2/\gamma_2$ with this γ_2 and the above q. We now know approximate values for $E, q, \gamma_1, \delta_1, \epsilon_1, \gamma_2, \delta_2$ and ϵ_2 as we increase r_2^2 from 0, but must make sure that the new zeros and poles we are creating pull apart in the correct manner. The argument is precisely the same as that used to establish (6.2), but because $a_2 < 0$ while we had $a_1 > 0$ before, and (3.2) shows that the sign of the residue of $g(\zeta)$ at $\zeta = \gamma_j$ depends on the sign of a_j, we find that we must have

$$\delta_2 < \epsilon_2 < q^2/\gamma_2 \qquad \text{if } r_2^2 > 0, \tag{6.4}$$

the opposite inequalities to those in (6.2). Using estimates that respect (6.4), we can solve for a small positive value of r_2^2, and then path-follow up to the value $r_2^2 = (0.8)^2$ needed in figure 12.

We have discussed the strategy used to produce the figures at some length because it *is* necessary to obtain reasonable estimates to ensure the convergence of the iteration routine that solves the equations, particularly when the conformal map to be found involves considerable distortion. In this respect, it is helpful to remember that formula (3.17) *is* unchanged if we replace ϵ_j by $q^2/\bar{\epsilon}_j$: our development distinguishes between these zeros of $g(\zeta) + r^2$ only by requiring that it be ϵ_j that coincides with δ_j when the mapping degenerates, rather than $q^2/\bar{\epsilon}_j$. A cavalier approach to solving the equations generally fails to secure convergence, but one can also converge to solutions that do not satisfy (6.2), (6.3) or (6.4), for example, but which are still acceptable because of this inherent indeterminacy. For $N > 1$, one should also bear in mind that our choice of subscripts among the parameters has been made by demanding that both δ_j and ϵ_j tend to $q^2/\bar{\gamma}_j$ in a degenerate situation, with γ_j itself linked to a particular injection point $z = a_j$ by (2.1) and (2.5), for each $j = 1, 2, \ldots, N$. A less rational approach to the numerical work may still produce suitable solutions, but with these parameters permuted.

7. The disappearing air hole

In this section, we consider the situation as the air hole vanishes and the doubly connected region occupied by the fluid becomes simply connected. Mathematically, this corresponds to the limit $q \to 0$ in the analysis. This stage of the motion is of particular interest in many applications, when a prior knowledge of the location of the point where the air hole disappears can be vital.

We consider first the simplest case $N = 1$, and suppose a_1 to be real and positive, so that the parameters γ_1, δ_1 and ϵ_1 are also real and positive. Thus our present discussion is directly relevant for figures 1, 3, 4 and 10. In these figures we see that the only zero $\zeta = \delta_1$ of $f(\zeta)$ in the annulus $q^2 < |\zeta| \leqslant 1$ has moved into the annulus $q < |\zeta| < 1$ well before the hole disappears, and δ_1 tends to some non-zero limit as $q \to 0$. Trivially, γ_1 tends to some non-zero limit too: we still have $\zeta = \gamma_1$ as the image of $z = a_1$ under the degenerate form of the map, and we must have $q < \gamma_1 < 1$ throughout. On the other hand, ϵ_1 and q^2/ϵ_1 are the two zeros of $g(\zeta) + r^2$ in the annulus $q^2 < |\zeta| \leqslant 1$ and the initial injection into the annulus produces parameters satisfying $\epsilon_1 < \delta_1 < q < q^2/\epsilon_1$; see (6.2). Now δ_1 can never coincide with either ϵ_1 or q^2/ϵ_1, for δ_1 is a zero of $g(\zeta)$ while ϵ_1 and q^2/ϵ_1 are zeros of $g(\zeta) + r^2$, so that while δ_1 moves into the annulus $q < |\zeta| < 1$ as the origin becomes covered by fluid, ϵ_1 must

remain in the annulus $q^2 < |\zeta| < q$. In particular, $\epsilon_1 \to 0$ as $q \to 0$, but q^2/ϵ_1 tends to some non-zero limit less than 1.

If we take the form (3.17) for the map (with $N = 1$ and all the parameters real) and let $q \to 0$ and $\epsilon_1 \to 0$ so that $q^2/\epsilon_1 \to \epsilon_1^*$, say, and continue to use the labels E, γ_1 and δ_1 for the limiting values of these parameters, we find that the limiting form of the map is

$$f(\zeta) = E\,\frac{(\zeta - \delta_1)(1 - \epsilon_1^*\zeta)}{(1 - \delta_1\zeta)(1 - \gamma_1\zeta)}. \tag{7.1}$$

Thus $f(\zeta)$ becomes a rational function of degree 2, which is what we should have expected: in this limit, we have a simply connected region whose Cauchy transform $h_e(z)$ has just 2 simple poles at $z = 0$ and $z = a_1$, according to (1.7), and this is just the situation treated as an example by Richardson (1972) with the map now involving the whole unit disc $|\zeta| < 1$. In that paper, the normalization used for the map was different for, with simply connected regions being discussed, we were able to demand that the origins in the z-plane and ζ-plane should correspond. Here we find that $f(0) = -E\delta_1$, and this tells us the location of the point at which the hole disappears once we know the parameters in (7.1).

These parameters are determined, of course, as solutions of the appropriate degenerate forms of our equations. These will not be written down for the case $N = 1$ we are discussing, because they are just special cases of the forms for general N we will give later, but we do make some comments on their use: note that formula (7.1) has one fewer parameter in it than has (3.17) for $N = 1$, since we have let $q \to 0$.

To obtain the outlines of the doubly connected blobs appearing in figures 1, 3 and 4, we solve for the five real parameters E, q, γ_1, δ_1 and ϵ_1 using five real equations, one of which is (4.2), for given increasing values of r_1^2. For the disappearing scenario, q drops out as a parameter but r_1^2 becomes an unknown (we do not know *a priori* how much we must inject before the hole disappears) so we still have five real unknowns, and the five real equations we need are the degenerate forms of all five used earlier, including (4.2).

To obtain the outlines of the doubly connected blobs appearing in figure 10, we solve for the five real parameters E, q, γ_1, δ_1 and ϵ_1 using five real equations, one of which is (4.1), for given decreasing values of the hole area. For the disappearing scenario, q drops out as a parameter and only four remain to be found, and the four real equations we need are the degenerate forms of only four of those used earlier, for (4.1) has become redundant.

In figures 1, 3 and 4, three outlines of the simply connected blob as it continues to grow after the hole has disappeared are drawn too. These are also maps of the unit circle $|\zeta| = 1$ given by rational functions of degree 2; the equations for determining this stage of the motion are given by Richardson (1972).

We now consider the development as the hole disappears and $q \to 0$ when $N > 1$, the situation in figures 13 and 15. As for $N = 1$, when the fluid moves to cover the origin, a zero of $f(\zeta)$ moves into the annulus $q < |\zeta| < 1$, but $f(\zeta)$ now has $N > 1$ zeros in $q^2 < |\zeta| < 1$ at $\zeta = \delta_j$ for $j = 1, 2, \ldots, N$, and only one of these can cross $|\zeta| = q$. If we have path-followed from an initial annular state, thus linking δ_j to the injection point $z = a_j$ with the same j, we discover which zero it is that moves into $q < |\zeta| < 1$, and this tends to some non-zero limit. By renumbering, if necessary, we suppose this zero to be δ_1. If it is only the degenerate situation that concerns us, this becomes a definition: δ_1 is *the* zero that tends to a non-zero limit. For all the

other zeros we must have $\delta_j \to 0$ as $q \to 0$ for $j = 2, \ldots, N$, since $f(\zeta)$ is always univalent in $q < |\zeta| < 1$ and can therefore have only one zero there, but $q^2/\overline{\delta}_j$ *does* tend to a non-zero limit that is less than 1 in modulus. Similarly, $\epsilon_j \to 0$ as $q \to 0$ for $j = 1, 2, \ldots, N$, but $q^2/\overline{\epsilon}_j$ tends to a non-zero limit that is less than 1 in modulus.

If $N > 1$, it is possible to have a situation in which the air hole vanishes at the origin, and then $\delta_j \to 0$ as $q \to 0$ for *all* $j = 1, 2, \ldots, N$. This can be thought of as a special case of the above in which we allow 0 to be a limit of δ_1 as $q \to 0$. However, the limit $\delta_1 \to 0$ needs to be examined rather carefully in some of the equations to follow. In fact, the obvious instances where the hole vanishes at the origin involve a symmetric arrangement of injection points and it is sensible to exploit that symmetry from the beginning: it is certainly foolish to single out one zero for special treatment, as we must in general. In the following presentation, we suppose that the hole vanishes at some point other than the origin. In physical terms, of course, there can be no qualitative difference between a motion in which the air hole vanishes *exactly* at the origin, and one where it *almost* does so.

If we take the form (3.17) for the map and let $q \to 0$, let $\delta_j \to 0$ so that $q^2/\delta_j \to \delta_j^*$, say, for $j = 2, \ldots, N$, let $\epsilon_j \to 0$ so that $q^2/\epsilon_j \to \epsilon_j^*$, say, for $j = 1, 2, \ldots, N$, and continue to use E, γ_j and δ_1 for the limiting values of these parameters, we find that the limiting form of the map is

$$f(\zeta) = E\,\frac{\zeta - \delta_1}{1 - \overline{\delta}_1\zeta} \prod_{j=1}^{N} \frac{1 - \epsilon_j^*\zeta}{1 - \overline{\gamma}_j\zeta}\,; \tag{7.2}$$

we note that (7.2) reduces to (7.1) for $N = 1$ when we suppose the parameters to be real. It also gives us the same simple result for the point where the hole disappears: it vanishes at

$$f(0) = -E\delta_1. \tag{7.3}$$

Equation (7.2) expresses $f(\zeta)$ as a rational function of degree $N + 1$, and this is again what we expect. We have a simply connected region whose Cauchy transform $h_e(z)$ has $N+1$ simple poles, as in (1.7), and the routine of Richardson (1972) shows that such a region is obtained from the unit disc $|\zeta| < 1$ by a map with this structure.

We now consider the degenerate form of the equations to be solved as $q \to 0$. Equation (2.1) needs no comment, for we use it as it stands with $f(\zeta)$ given by (7.2). Equation (3.19) becomes

$$\overline{\gamma}_1\delta_1 \frac{(1 - \delta_1\epsilon_j^*)(\epsilon_j^* - \overline{\delta}_1)}{(1 - \gamma_1\epsilon_j^*)(\epsilon_j^* - \overline{\gamma}_1)} \prod_{k=2}^{N} \frac{\overline{\gamma}_k(\epsilon_j^* - \delta_k^*)(1 - \overline{\delta}_k^*\epsilon_j^*)}{\delta_k^*(1 - \gamma_k\epsilon_j^*)(\epsilon_j^* - \overline{\gamma}_k)} = -\frac{r^2}{E^2} \quad \text{for } j = 1, 2, \ldots, N. \tag{7.4}$$

Equation (3.20) becomes

$$\prod_{k=1}^{N} \frac{\epsilon_k^*}{\overline{\epsilon}_k^*}(1 - \gamma_1\epsilon_k^*)(\overline{\epsilon}_k^* - \gamma_1) = \overline{\gamma}_1\overline{\delta}_1(\delta_1 - \gamma_1)(1 - \gamma_1\overline{\delta}_1) \prod_{k=2}^{N} \frac{\overline{\gamma}_k}{\overline{\delta}_k^*}(1 - \gamma_1\delta_k^*)(\overline{\delta}_k^* - \gamma_1). \tag{7.5}$$

Equation (3.21) becomes

$$E^2\,\frac{(\gamma_j - \overline{\epsilon}_j^*)(1 - \gamma_j\epsilon_j^*)}{1 - \overline{\gamma}_j\gamma_j}\,\frac{f'(\gamma_j)}{f(\gamma_j)} \prod_{\substack{k=1 \\ k\neq j}}^{N} \frac{(\gamma_j - \overline{\epsilon}_k^*)(1 - \gamma_j\epsilon_k^*)}{(1 - \overline{\gamma}_k\gamma_j)(\gamma_j - \gamma_k)} = r_j^2 \quad \text{for } j = 1, 2, \ldots, N. \tag{7.6}$$

Equation (4.1) is never relevant in these circumstances, and the form of (4.2) we need follows directly from that given: just set $\zeta_q = 0$ therein. The correct equations for the special case $N = 1$ are obtained from (7.4), (7.5) and (7.6) if we interpret empty products as having the value 1, as usual.

We note that, while the parameters δ_j^* for $j = 2, \ldots, N$ do not appear in the expression we now have for the map $f(\zeta)$ in (7.2), they are inextricably bound up in our equations. A count of the unknowns and equations that arise in the various problems we may consider when $N > 1$ shows that we have the correct number of equations, just as we had when $N = 1$: remember that it is only the real part of (7.5) that we need.

In the examples illustrated in figures 13 and 15, it was found to be the zero associated with the larger disc that had a non-zero limit, while the zero associated with the smaller disc approached the origin as $q \to 0$. This seems to pose a dilemma: what happens when the discs are the same size? In fact, we have an instance of a classic symmetry-breaking scenario. With the discs of equal radius, there is a line of symmetry in both the z-plane and the ζ-plane. The zeros move on paths that are symmetric with respect to this line in the ζ-plane until they coalesce on it while they are still both in the annulus $q^2 < |\zeta| < q$. At this instant, of course, they lose their individual identities, and their subsequent motion is confined to this line of symmetry, with one moving to the origin and the other staying away from it. If we have two discs of almost equal radii, the zeros never coalesce, but both the one from the smaller disc that approaches the origin and the one from the larger disc that stays away from it move on paths close to those on which they move when symmetry prevails.

8. The cusped configurations

Before considering any of the cusped configurations, we recall that our mapping function $f(\zeta)$ is always meromorphic for $\zeta \neq 0$, and note that the poles play no part in the formation of the type of cusps we are considering. (They do have a role to play in the 'double-cusp' configurations that arise as blobs are absorbed or disgorged.) As a cusp appears in a free boundary corresponding to $|\zeta| = q$, say, the function $f(\zeta)$ remains analytic in a full neighbourhood of the circle $|\zeta| = q$, the cusp being produced by a zero of $f'(\zeta)$ that moves to this circle from $|\zeta| < q$.

Consider, now, the approach to the configuration in the left-hand sketch of figure 2. With the symmetry, we have five real parameters E, q, γ_1, δ_1 and ϵ_1 to solve for and five real equations (2.1), (3.19), (3.20), (3.21) and (4.2) to satisfy as r_1^2 decreases from 0. As we near the cusped configuration, we need to find the value of r_1^2 to which it corresponds; we add the equation $f'(q) = 0$ to our set of equations (it is just one real equation because of the symmetry) and are thus able to solve for the extra unknown r_1^2 as well, to find the parameter values needed for this sketch.

For the right-hand sketch in figure 2 the procedure is similar, but the extra equation to be added is $f'(1) = 0$ because the cusp is now in the outer boundary.

For the middle sketch in figure 2 we need to locate the suction point so that cusps appear simultaneously in both boundaries. We now add in two extra equations $f'(q) = 0$ and $f'(1) = 0$ to enable us to solve for the two extra unknowns a_1 and r_1^2.

The calculations for figure 2 are simplified by the symmetry. Suppose we had a similar situation lacking symmetry with $N > 1$, and were path-following a solution

PHILOSOPHICAL TRANSACTIONS OF THE ROYAL SOCIETY A MATHEMATICAL, PHYSICAL & ENGINEERING SCIENCES

with suction at $z = a_1$, so r_1^2 is decreasing. We see a cusp beginning to appear in the inner boundary and wish to determine its location and the value of r_1^2 when it materializes. It corresponds to some point $\zeta = q\mathrm{e}^{\mathrm{i}\theta_0}$ on $|\zeta| = q$, and we need to add the equation $f'(q\mathrm{e}^{\mathrm{i}\theta_0}) = 0$ to our set; this single complex equation now comprises two real equations through its real and imaginary parts, thus allowing the two extra unknowns θ_0 and r_1^2 to be found—and having found θ_0, the cusp is at $z = f(q\mathrm{e}^{\mathrm{i}\theta_0})$.

We have recounted the simple logical steps required to produce figure 2 in some detail because we must adopt a similar approach for figure 15, and this proves not to be so straightforward. We consider figure 14 first.

We move through the non-touching configurations in figure 14, solving our set of equations as we decrease the hole area. Nearing the touching configuration, we wish to determine precisely the parameter values that prevail at contact. The point of contact in the z-plane corresponds to two points in the ζ-plane, say $\zeta = q\mathrm{e}^{\mathrm{i}\theta_1}$ and $\zeta = q\mathrm{e}^{\mathrm{i}\theta_2}$, where we may suppose that $0 < \theta_1 < \theta_2 < 2\pi$. When touching, we evidently have

$$f(q\mathrm{e}^{\mathrm{i}\theta_1}) = f(q\mathrm{e}^{\mathrm{i}\theta_2}), \tag{8.1}$$

but this equation is not sufficient to fix the geometry. In fact, one may envisage mathematical solutions a little beyond the moment of contact illustrated in figure 14, with the fluid regions actually overlapping, and there are then *two* pairs of values (θ_1, θ_2) that satisfy (8.1). The solution we seek is just one from a continuum of solutions present when we add only (8.1) to our earlier set of equations. The extra condition we need to ensure that the inner boundary does indeed *touch* itself at the point in question is that the normals at the points corresponding to $\zeta = q\mathrm{e}^{\mathrm{i}\theta_1}$ and $\zeta = q\mathrm{e}^{\mathrm{i}\theta_2}$ should have opposite directions. For present purposes, this condition can be conveniently written in terms of the arguments of complex numbers as

$$\arg\{\mathrm{e}^{\mathrm{i}\theta_2} f'(q\mathrm{e}^{\mathrm{i}\theta_2})\} = \arg\{\mathrm{e}^{\mathrm{i}\theta_1} f'(q\mathrm{e}^{\mathrm{i}\theta_1})\} + \pi. \tag{8.2}$$

We now have the equations we need. Adding equation (8.1), which is a complex equation with 2 real ones as its real and imaginary parts, and the real equation (8.2) to our set, we have the 3 extra real equations we need to find the 3 extra real unknowns θ_1, θ_2 and the hole area as the inner boundary touches itself.

Now consider figure 15, which we must view as a limiting form of figure 14. To obtain this, we know that we must choose the radius of the upper-left circular disc, say r_2, carefully; if r_2 does not have precisely the correct value, we obtain motions as in figure 13 or figure 14. The cusp in figure 15 corresponds to some point $\zeta = q\mathrm{e}^{\mathrm{i}\theta_0}$ in the ζ-plane so that, as for figure 14, there are 3 extra real unknowns θ_0, r_2 and the hole area to be determined to locate the cusped configuration. We thus need 3 extra real equations and they evidently arise as the limiting forms of equations (8.1) and (8.2), this limit involving $\theta_1 \to \theta_0$ and $\theta_2 \to \theta_0$. That (8.1) leads to the expected, familiar, condition $f'(q\mathrm{e}^{\mathrm{i}\theta_0}) = 0$ for a cusp is easy to see, but the limiting form of condition (8.2) is less obvious. Indeed, the result we need is *not* a consequence of (8.2) alone, but of (8.1) and (8.2) together. Consider, again, the mathematical solution reached a little beyond the moment of contact in figure 14. This has values of θ_1 and θ_2 that satisfy (8.2), and we can imagine a limit of *this* configuration tending to a cusped one with the overlap maintained throughout, but it is not this limit we need. The cusped configuration in figure 15 is thus one of a continuum of solutions present in the parameter space when we add only $f'(q\mathrm{e}^{\mathrm{i}\theta_0}) = 0$ to our set of equations. As the foregoing suggests, the limit we seek is the only one from the above continuum

that yields a univalent map; we will return to this point later, but concentrate on finding the required extra condition from (8.1) and (8.2) for the moment.

We need to consider variable mappings as the touching configuration in figure 14 changes, with the point of contact moving towards the upper-right lobe of the air hole until this lobe disappears as the cusp forms. We denote this mapping by $z = f(\zeta, \varepsilon)$ and suppose the limit $\varepsilon \to 0$ to correspond to approach to the cusped configuration; thus we are seeking conditions involving $f(\zeta, 0) \equiv f(\zeta)$, with $f(\zeta)$ the function giving the map for figure 15. It would appear that we should take either $\varepsilon = \theta_1 - \theta_0$ or $\varepsilon = \theta_2 - \theta_0$, but this makes the analysis unnecessarily complicated; we take $\varepsilon = \theta_2 - \theta_1$. In fact, the need to introduce θ_0 arises only because we have chosen to normalize our mappings by supposing E in (3.17) to be real and positive, and it is difficult to link this global condition to the local analysis we face. Since it is a local condition we seek and it cannot depend on the particular normalization used, we could take $\theta_0 = \theta_1$ for present purposes, but will not do so.

With our modified notation for the varying maps and $\varepsilon = \theta_2 - \theta_1$, equation (8.1) is

$$f(q\mathrm{e}^{\mathrm{i}\varepsilon}\mathrm{e}^{\mathrm{i}\theta_1}, \varepsilon) = f(q\mathrm{e}^{\mathrm{i}\theta_1}, \varepsilon). \tag{8.3}$$

Now expand both sides of (8.3) in powers of ε: recall the comments made at the beginning of this section concerning the analytic behaviour of the mappings. From the $O(\varepsilon)$ term in (8.3) we find $f'(q\mathrm{e}^{\mathrm{i}\theta_1}, 0) = 0$, where $f'(\zeta, \varepsilon)$ denotes the derivative of $f(\zeta, \varepsilon)$ with respect to its first argument. In terms of the notation relevant for figure 15, this is

$$f'(\zeta) = 0 \qquad \text{for } \zeta = q\mathrm{e}^{\mathrm{i}\theta_0}. \tag{8.4}$$

This is the expected cusp condition, but we also need other consequences of (8.3). Comparing the $O(\varepsilon^2)$ and $O(\varepsilon^3)$ terms in this, we obtain two identities, which we will not record, that relate derivatives of $f(\zeta, \varepsilon)$ with respect to its first and second arguments when evaluated for $\zeta = q\mathrm{e}^{\mathrm{i}\theta_1}$ and $\varepsilon = 0$. Using these, we find that

$$\frac{\mathrm{e}^{\mathrm{i}\theta_2} f'(q\mathrm{e}^{\mathrm{i}\theta_2}, \varepsilon)}{\mathrm{e}^{\mathrm{i}\theta_1} f'(q\mathrm{e}^{\mathrm{i}\theta_1}, \varepsilon)} = -1 - \mathrm{i}\varepsilon \left\{ 1 + \frac{q\mathrm{e}^{\mathrm{i}\theta_1}}{3} \frac{f'''(q\mathrm{e}^{\mathrm{i}\theta_1}, 0)}{f''(q\mathrm{e}^{\mathrm{i}\theta_1}, 0)} \right\} + O(\varepsilon^2). \tag{8.5}$$

Now an alternative interpretation of condition (8.2) in our notation requires the expression on the left-hand side of (8.5) to be real and negative, and to ensure that this is so to $O(\varepsilon)$ we see that the expression in braces in (8.5) must be purely imaginary. Thus the condition we need to compute for figure 15 is

$$\mathrm{Re}\left\{ \zeta \frac{f'''(\zeta)}{f''(\zeta)} \right\} = -3 \qquad \text{for } \zeta = q\mathrm{e}^{\mathrm{i}\theta_0}; \tag{8.6}$$

note that we must have $f''(q\mathrm{e}^{\mathrm{i}\theta_0}) \neq 0$ as we are dealing with univalent maps.

Adding the 3 real equations furnished by the real and imaginary parts of equation (8.4) and the real equation (8.6) to our set, we have sufficient equations to solve for the 3 extra real unknowns θ_0, r_2 and the hole area.

Equation (8.6), in an appropriate guise, is needed to compute the geometric data necessary to produce a motion that passes *through* a cusped configuration in other settings, such as those mentioned at the end of § 5, and it can be related to other features of such motions. If we calculate the curvature κ of the inner boundary curve at the point corresponding to $\zeta = q\mathrm{e}^{\mathrm{i}\theta}$ near the point corresponding to $\zeta_0 = q\mathrm{e}^{\mathrm{i}\theta_0}$, we

find that

$$\kappa = \frac{1}{2|\zeta f'(\zeta)|}\left[3 + \mathrm{Re}\left\{\zeta_0 \frac{f'''(\zeta_0)}{f''(\zeta_0)}\right\} + O(\theta - \theta_0)\right]. \tag{8.7}$$

Thus, if (8.4) holds but (8.6) does not, we have $\kappa \to \pm\infty$ as $\theta \to \theta_0$, the sign depending on the sign of the $O(1)$ term within square brackets in (8.7). The correspondence of signs here depends on the sign convention in the definition of κ but that is not relevant for us here, and we see from this an alternative interpretation of condition (8.6): it selects for us from the continuum of solutions obtained if we add only condition (8.4) to our set of equations that solution yielding a univalent map, for we know that this univalent map only has non-univalent ones nearby.

When both (8.4) and (8.6) hold, we see that (8.7) implies that the curvature is bounded in a neighbourhood of the cusp. In fact, further considerations, to be mentioned briefly shortly, imply that the curvature then tends to 0 as the cusp is approached.

If we perform a local expansion about a cusp using appropriately scaled and oriented Cartesian coordinates (X, Y) with origin at the cusp, and suppose (8.4) to hold but not (8.6), we find that the boundary shape is described locally by

$$Y \sim \pm\left[3 + \mathrm{Re}\left\{\zeta_0 \frac{f'''(\zeta_0)}{f''(\zeta_0)}\right\}\right] X^{3/2} \qquad \text{as } X \to 0+, \tag{8.8}$$

where $\zeta_0 = q\mathrm{e}^{\mathrm{i}\theta_0}$ is the point in the ζ-plane corresponding to the cusp. Thus, in the terminology of Howison (1986), we have a 3/2-power cusp if condition (8.6) is not satisfied. Imposing condition (8.6) ensures that we have a cusp of higher power than 3/2, and a deeper examination shows that its power must be at least 5/2. We note that, in agreement with earlier comments, a 3/2-power cusp has unbounded curvature in its neighbourhood, while the curvature tends to 0 as a 5/2-power cusp is approached.

9. Concluding remarks

The primary aim of this paper has been to present a procedure for the solution of a particular class of free boundary problems arising in Hele-Shaw flow. In spite of the many specific examples given in § 5, we make no claim to have mentioned all the interesting phenomena that can occur. One can, of course, combine features from different examples here, and the possibilities multiply when we exploit other ideas that appear in Richardson (1996*a*,*b*). For example, all the isolated blobs that feature in the motions in § 5 are circular, but we can add further injection or suction points to give them other shapes, as in the earlier works. By drawing on experience in similar situations, one can answer some of the questions one might pose concerning such variations. What happens if the circular disc in figure 8 is replaced by a non-convex body in some orientation? What happens in figures 11 and 12 if we begin with an initial waist on the left created by a small amount of initial suction, instead of a bulge? What happens in these figures if it is suction we apply on the right instead of injection? By using shapes that are other than circular in figure 14, can we arrange that the air hole splits into *more* than two pieces at some instant, with the inner boundary touching itself at *more* than one point? Could we use a limiting form of such an arrangement to produce a motion that passes through a state with a cusp of a power higher than 5/2? Could the inner boundary be made to touch

PHILOSOPHICAL TRANSACTIONS OF THE ROYAL SOCIETY A MATHEMATICAL, PHYSICAL & ENGINEERING SCIENCES

itself simultaneously along an entire curve, and can we contemplate a limiting form of this? Recall the earlier remarks that the phenomenon of motion passing through a cusped state, as presented in figure 15, can also be demonstrated in simpler settings, though it is the sequence of figures 13, 14 and 15 that has provoked some of these questions.

Any initial doubly connected configuration can be approximated as closely as we wish by members of the family discussed here but, because the problems are ill-posed in the sense that they are sensitive to changes in the initial conditions, this is of limited use. Indeed, if we are content to work with such approximations, the basic annulus itself can be formed as accurately as we please by injecting uniformly at a sufficient number of points uniformly distributed round a circle—but no such approximation predicts even the trivial expansion of the annulus correctly. To deal with more general doubly connected configurations than those considered here, we must solve a functional equation more general than that in (2.7). When the connectivity of the region occupied by fluid is greater than two, a situation towards which we have been driven in some of the examples, the analysis requires a further generalization.

We should emphasize that our mathematical model has made the simple assumption of constant pressure along each free boundary, and it will predict the correct behaviour of a given physical system only when this is a reasonable assumption. With surface tension present, it must eventually become invalid as the curvature of the free boundary increases. Nevertheless, it would be interesting to see how closely some of the phenomena exhibited by the examples could be reproduced in an experiment.

The numerical computations required for this paper were performed using *Mathematica* (Version 2), and its graphics facilities were employed to produce the figures.

Appendix A. The functions $F(z)$ and $G(z)$

With present applications in mind, we suppose the parameter q to be real and such that $0 < q < 1$. In fact, our definitions are still applicable if q is complex with $0 < |q| < 1$, and there is some mathematical interest in considering this generalization; if we were concerned purely with theoretical properties of the functions, we would undoubtedly replace q^2 by q throughout too.

We define $F(z) \equiv F(z;q)$ for $z \neq 0$ by

$$F(z) = (1-z)\prod_{m=1}^{\infty}(1-q^{2m}z)\prod_{n=1}^{\infty}(1-q^{2n}/z). \tag{A 1}$$

As here, we do not explicitly mention the dependence of $F(z)$ on q in our notation for we will not need to consider the behaviour of $F(z)$ under a transformation of this parameter. $F(z)$ is an analytic function of z for all $z \neq 0$, and has zeros at, and only at, the points $z = q^{2n}$ with n an integer, and they are all simple zeros. The origin $z = 0$ is a limit point of these zeros, and is therefore an essential singularity of $F(z)$.

Straightforward reorganizations of the terms in the products in (A 1) show that

$$F(1/z) = -(1/z)F(z) \tag{A 2}$$

and

$$F(q^2z) = -(1/z)F(z). \tag{A 3}$$

We define $G(z) \equiv G(z;q)$ by

$$G(z) = \frac{\prod_{n=1}^{\infty}(1-q^{2n+2}/z)^n}{\prod_{m=1}^{\infty}(1-q^{2m-2}z)^m}, \tag{A 4}$$

so that $G(z)$ is meromorphic for $z \neq 0$. It has a zero of order n at $z = q^{2n+2}$ for all integers $n \geqslant 1$, and a pole of order n at $z = q^{2-2n}$ for all integers $n \geqslant 1$, and no other zeros or poles in $|z| > 0$. The zeros have the origin $z = 0$ as a limit point, so that this is an essential singularity of $G(z)$, while the limit point of the poles is at infinity. Note that the entire annulus $q^4 < |z| < 1$ is free of both zeros and poles.

A simple consequence of (A 4) is that

$$G(q^2z)G(q^2/z) = 1, \tag{A 5}$$

but the crucial result we need for our purposes requires a little more manipulation. Replacing z by q^2z in (A 4) and regrouping the terms in the products, we find that

$$G(q^2z) = F(z)G(z). \tag{A 6}$$

In fact, our function $F(z)$ can be expressed in terms of the standard theta functions. Using the notation of Whittaker & Watson (1927), we have

$$F(z) = -\mathrm{i}P^{-1}q^{-1/4}\mathrm{e}^{\pi\mathrm{i}v}\vartheta_1(\pi v, q), \tag{A 7}$$

where

$$z = \mathrm{e}^{2\pi\mathrm{i}v} \quad \text{and} \quad P = \prod_{n=1}^{\infty}(1-q^{2n}). \tag{A 8}$$

The function $G(z)$ can also be directly related to $F(z)$, and therefore to the theta functions. We have

$$G(q^2z) = \exp\left\{\int_1^z \frac{F_{q^2}(z)}{F(z/q^2)}\,\mathrm{d}z\right\}, \tag{A 9}$$

where $F_{q^2}(z)$ denotes the partial derivative of $F(z)$, as defined in (A 1), with respect to q^2.

The definitions (A 1) and (A 4) display the essential features of the functions $F(z)$ and $G(z)$ concisely, and *Mathematica* is able to compute their values directly from these; formulae (A 7), (A 8) and (A 9) were not used. In fact, the numerical work for this paper also required that values for the derivatives of $F(z)$ and $G(z)$ with respect to z up to order three be computed, and *Mathematica* did this using the formulae one obtains by differentiating (A 1) and (A 4) logarithmically with no difficulty.

The functions $F(z)$ and $G(z)$ have a large number of properties, representations, special values, etc. that we do not present here. All we need is recorded above, or follows very easily from these results.

Appendix B. Loxodromic functions

As in Appendix A, we suppose that q is real and $0 < q < 1$. For our purposes, a loxodromic function $l(z)$ is a meromorphic function for $z \neq 0$ that satisfies

$$l(q^2z) = l(z)\,; \tag{B 1}$$

we are using the nomenclature of Valiron (1966), and our presentation in this appendix is modelled on that in this reference.

Since a rectangle and a concentric circular annulus furnished with a radial cut are related by an appropriate exponential map, there is a close connection between loxodromic functions and elliptic functions; indeed, Valiron (1966) presents the classical theory of elliptic functions, in both the Jacobian and Weierstrassian forms, as a development of the theory of loxodromic functions. Some of the results we record below may be more familiar in the elliptic setting, but we do not assume such familiarity.

The behaviour of $l(z)$ is determined everywhere if we know it in the annulus $q^2 < |z| \leqslant 1$; we refer to this as the *fundamental annulus*. If $z = b$ is a zero of $l(z)$ in this annulus, then all the points $z = q^{2n}b$ for n any integer are also zeros of the same order; we call such zeros *equivalent*. If $z = c$ is a pole of $l(z)$ in the fundamental annulus, then all the points $z = q^{2n}c$ for n any integer are also poles of the same order; we call such poles *equivalent*. More generally, we may speak of *equivalent points*, with a meaning that is evident.

If no pole lies on the boundary of the fundamental annulus, we can integrate $l(z)/z$ round this boundary (with the usual convention that the boundary is to be traversed in a direction that places the domain it bounds to the left) and find the result to be zero. Thus the sum of the residues of $l(z)/z$ at its poles within this annulus is then zero. This final result is still correct when poles *do* lie on the boundary of the fundamental annulus, but we must use a slight deformation of the contour of integration to prove it. Such technical problems caused by the awkward positioning of special points occur frequently in the theory of loxodromic and elliptic functions, and are dealt with in a similar manner. In our subsequent discussion, we will not comment on such details.

From the above, a loxodromic function cannot have just one simple pole in the fundamental annulus. If a loxodromic function has *no* poles in the fundamental annulus, then (B 1) implies that it is bounded for $z \neq 0$, so the origin is actually a removable singularity: the only loxodromic functions with no poles are the constants.

Integrating $l'(z)/l(z)$ round its boundary, we find that a loxodromic function must have an equal number of zeros and poles in the fundamental annulus—and this number must be finite—provided we count zeros and poles according to multiplicity. Suppose, then, that $z = b_1, b_2, \ldots, b_m$ are the zeros of $l(z)$ in the fundamental annulus, and $z = c_1, c_2, \ldots, c_m$ are its poles there, where a given point appears here a number of times equal to the order of the zero or pole. Consider the function

$$M(z) = \frac{F(z/b_1)F(z/b_2)\ldots F(z/b_m)}{F(z/c_1)F(z/c_2)\ldots F(z/c_m)} \tag{B 2}$$

where $F(z)$ is the function defined in (A 1). This function $M(z)$ has the same zeros and poles as $l(z)$, so that

$$N(z) = \frac{M(z)}{l(z)} \tag{B 3}$$

is analytic for $z \neq 0$ with neither zeros nor poles in $|z| > 0$. Now (A 3) implies that

$$M(q^2 z) = \lambda M(z) \qquad \text{where} \qquad \lambda = \frac{b_1 b_2 \ldots b_m}{c_1 c_2 \ldots c_m}, \tag{B 4}$$

so that we have

$$N(q^2 z) - \lambda N(z) \equiv 0 \qquad \text{for } z \neq 0. \tag{B 5}$$

But $N(z)$ can be expressed as a Laurent series for $z \neq 0$, say

$$N(z) = \sum_{n=-\infty}^{+\infty} d_n z^n,$$

so that (B 5) is

$$\sum_{n=-\infty}^{+\infty} d_n(q^{2n} - \lambda)z^n \equiv 0 \qquad \text{for } z \neq 0,$$

whence

$$d_n(q^{2n} - \lambda) = 0 \qquad \text{for all } n. \tag{B 6}$$

Now $N(z)$ does not vanish identically, so we must have $d_p \neq 0$ for some p, whence $\lambda = q^{2p}$ or

$$\frac{b_1 b_2 \dots b_m}{c_1 c_2 \dots c_m} = q^{2p}. \tag{B 7}$$

(Note that this restriction also implies the result already mentioned: we cannot have $m = 1$.) We have reached this conclusion by starting with all the b_i and c_i in the fundamental annulus. But if $p \neq 0$ in (B 7), we may replace one (or more) of the zeros b_i or poles c_i by an equivalent zero or pole to arrange that we *do* have $p = 0$ in (B 7); that is,we can choose representatives for the zeros and poles so that

$$b_1 b_2 \dots b_m = c_1 c_2 \dots c_m. \tag{B 8}$$

Then $\lambda = 1$ in (B 4), and (B 6) tells us that $d_n = 0$ for $n \neq 0$. Thus $N(z)$ is actually a non-zero constant $d_0 = 1/C$, say, and we have shown that our loxodromic function must have the representation

$$l(z) = C\frac{F(z/b_1)F(z/b_2)\dots F(z/b_m)}{F(z/c_1)F(z/c_2)\dots F(z/c_m)} \tag{B 9}$$

for some constant C.

We note an immediate consequence of (B 9): a loxodromic function is uniquely determined by giving its zeros and poles within the fundamental annulus *plus* its value at some other point there.

The loxodromic functions with which we deal in § 3 actually satisfy a further condition, in addition to (B 1): we have

$$l(z) = \overline{l(1/\bar{z})}. \tag{B 10}$$

The implications of this are easy to see, but important.

Firstly, (B 10) implies that, if b is a zero of $l(z)$ in the fundamental annulus, then so is $q^2/\bar{b}$. (If $|b| = 1$, then this statement requires modification because we have chosen our fundamental annulus to include the circle $|z| = 1$ but not the circle $|z| = q^2$; see the earlier comment concerning the awkward positioning of special points. If $|b| = q$, then $q^2/\bar{b} = b$, and the statement is to mean that such zeros must be of even order.) A similar comment applies to the poles. There must be an even number of zeros and poles, and these occur naturally in pairs. Condition (B 8) is now always attainable using zeros and poles in the fundamental annulus (modulo a technical proviso for zeros and poles on its boundary), and it reduces to a restriction on their arguments alone.

Secondly, with zeros and poles distributed so as to respect the above restrictions,

we see that (A 2) and the obvious property $F(z) = \overline{F(\overline{z})}$ imply that the constant C appearing in the representation (B 9) must be real if (B 10) holds. Thus a loxodromic function that also satisfies (B 10) is uniquely determined by giving its zeros and poles within the fundamental annulus, plus the *real part* of its value at some other point where that real part does not vanish.

Appendix C. Solution of a linear functional equation

We here obtain the solution $k(z)$ of the linear q^2-difference equation

$$k(q^2 z) = l(z)k(z), \tag{C 1}$$

where $l(z)$ is a given loxodromic function, as defined in Appendix A. We suppose $l(z)$ to be non-constant in our general discussion; see (C 3) below if it should happen to be a constant function. The analogous problem in the elliptic setting was considered by Picard (1878).

With $l(z)$ loxodromic, we know that it has the representation (B 9) when the zeros and poles are represented by b_i and c_i such that (B 8) is satisfied. If $l(z)$ also satisfies (B 10), we know that this has further implications for the zeros and poles, and the constant C in (B 9), but we need not concern ourselves with these in this appendix.

Define a function $m(z)$ that is meromorphic for $z \neq 0$ by

$$k(z) = \frac{G(z/b_1)G(z/b_2)\dots G(z/b_m)}{G(z/c_1)G(z/c_2)\dots G(z/c_m)}\, m(z), \tag{C 2}$$

where $G(z)$ is the function defined in (A 4). Using (A 6) and the representation for $l(z)$ in (B 9), we find that

$$m(q^2 z) = Cm(z). \tag{C 3}$$

We now proceed by examining three separate cases.

I. If $C = 1$, then (C 3) simply says that $m(z)$ is loxodromic, and therefore is either constant or has a representation of the form (B 9)—but note that the zeros and poles of $m(z)$ need bear no relation to those of $l(z)$.

II. If $C = q^{2n}$ for some integer $n \neq 0$, write

$$m(z) = z^n m_1(z).$$

Then we find that

$$m_1(q^2 z) = m_1(z),$$

so that $m_1(z)$ is loxodromic.

III. If C is not of either of the above forms, write

$$m(z) = \frac{F(z/\alpha_1)}{F(z/\alpha_2)}\, m_2(z), \tag{C 4}$$

where $F(z)$ is the function defined in (A 1), and α_1 and α_2 are constants to be chosen shortly. With the aid of (A 3), we find that

$$m_2(q^2 z) = \frac{\alpha_2 C}{\alpha_1}\, m_2(z),$$

so that choosing α_1 and α_2 in (C 4) to satisfy $\alpha_1 = \alpha_2 C$ implies that $m_2(z)$ is loxodromic.

We note that Cases I and II are effectively degenerate instances of Case III, and we can always write the solution of (C 1) with $l(z)$ given by (B 9) in the form

$$k(z) = \frac{G(z/b_1)G(z/b_2)\dots G(z/b_m)}{G(z/c_1)G(z/c_2)\dots G(z/c_m)} \frac{F(z/\alpha_1)}{F(z/\alpha_2)} L(z) \qquad (C\,5)$$

for some constants α_1 and α_2, and some loxodromic function $L(z)$. Case I corresponds to taking $\alpha_1 = \alpha_2$ while Case II corresponds to taking $\alpha_1 = q^{2n}\alpha_2$; in either case, the zeros of the function $F(z/\alpha_1)$ in the numerator of (C 5) cancel with those of the function $F(z/\alpha_2)$ in the denominator. In Case III, such a cancellation does not occur.

References

Hohlov, Y. E. & Howison, S. D. 1993 On the classification of solutions to the zero-surface-tension model for Hele-Shaw free boundary flows. *Q. Appl. Math.* **51**, 777–789.

Howison, S. D. 1986 Cusp development in Hele-Shaw flow with a free surface. *SIAM J. Appl. Math.* **46**, 20–26.

Picard, E. 1878 Sur une classe de fonctions transcendantes. *C.r. Acad. Sci. Paris* **86**, 657–660.

Richardson, S. 1972 Hele Shaw flows with a free boundary produced by the injection of fluid into a narrow channel. *J. Fluid Mech.* **56**, 609–618.

Richardson, S. 1994 Hele-Shaw flows with time-dependent free boundaries in which the fluid occupies a multiply-connected region. *Eur. J. Appl. Math.* **5**, 97–122.

Richardson, S. 1996*a* On the classification of solutions to the zero-surface-tension model for Hele-Shaw free boundary flows. *Q. Appl. Math.* (In the press.)

Richardson, S. 1996*b* Hele-Shaw flows with free boundaries driven along infinite strips by a pressure difference. *Eur. J. Appl. Math.* **7**, 345–366.

Valiron, G. 1966 *Cours d'analyse mathématique. I. Théorie des fonctions*, 3rd edn. Paris: Masson et Cie.

Whittaker, E. T. & Watson, G. N. 1927 *A course of modern analysis*, 4th edn. Cambridge University Press.

Received 5 September 1995; accepted 24 May 1996

PHILOSOPHICAL TRANSACTIONS OF THE ROYAL SOCIETY A MATHEMATICAL, PHYSICAL & ENGINEERING SCIENCES